Nematic phases of bent-core mesogens†

Christina Keith,[a] Anne Lehmann,[a] Ute Baumeister,[b] Marko Prehm[ab] and Carsten Tschierske*[a]

Received 6th November 2009, Accepted 23rd January 2010
First published as an Advance Article on the web 2nd March 2010
DOI: 10.1039/b923262a

Bent-core mesogens derived from 4-cyanoresorcinol with terminal alkyl chains have been synthesized and investigated by polarizing microscopy, XRD and electro-optical methods. Short chain compounds have exclusively nematic phases which can be cooled to ambient temperature. These nematic phases are similar to ordinary nematic phases with only nearest neighbour correlation (N) whereas long chain compounds form SmC-type cybotactic clusters and these cybotactic nematic phases (N_{cybC}) can be regarded as strongly fragmented SmC phases. The chain length dependent as well as temperature dependent structural transition from N to N_{cybC} is continuous and associated with a change of the position and intensity of the small angle scattering in the XRD patterns. Moreover, a temperature dependent stepwise transition from cybotactic nematic phases to different types of non-polar and tilted smectic phases ($SmC_{(I)}$ and $SmC_{(II)}$) is observed with a mesophase composed of elongated, but not yet fused cybotactic clusters (CybC) as an intermediate state of this transition. This improves the understanding of the nature and special properties of the nematic phases formed by bent-core molecules as well as their transition to smectic phases and it paves the way to new materials with spontaneous or field-induced biaxial nematic phases at ambient temperatures.

1. Introduction

Since its theoretical prediction[1] the biaxial nematic phase (N_b) has attracted a lot of attention[2,3] due to its special properties and potential for device applications, providing a way to much faster switching than possible with the presently used displays based on uniaxial nematic phases (N_u).[4] In the uniaxial nematic phases the molecular axes are oriented along the director **n**, whereas in the N_b phases there is an additional secondary director **m** which is perpendicular to **n** (Fig. 1a and b). In other words, in the N_u phase the molecules are rotationally disordered around the long axis whereas in the N_b phase this rotation is restricted to give a time averaged board-like shape of the molecules.

Though simulations predicted phase biaxiality[5–7] for several types of compounds, and numerous attempts have been undertaken, for example, with board-like molecules or by combining rod-like and disc-like units,[8,9] for none of these materials the biaxial nematic phase was proven unambiguously.[2,10] Hence, these classical approaches have failed so far and only recently biaxiality in nematic phases was proven for multipodes,[11] side chain polymers[12] and bent-core mesogens[13] by means of deuterium-NMR experiments and polarized IR absorption. Strangely, all these molecules showing phase biaxiality in nematic phases do not have a pronounced board-like shape and have structures which are far away from any optimal structure required theoretically for occurrence of biaxiality in a nematic phase.[4–7,14] Hence, it seems that other effects, such as intermolecular coupling and preorganization, are of significant importance and this led to a change of the paradigms in this field.[15] There are several experimental hints that in all systems with proven N_b phases the molecules are organized in clusters.[11–13,16] In these clusters local biaxiality can arise, but on a macroscopic scale these clusters are rotationally averaged so that no spontaneous biaxiality could be observed, for example, by optical methods (Fig. 1d). However, alignment of these clusters under the influence of external fields or at surfaces could lead to induced macroscopic biaxiality.[9,15,17–20] This induced biaxiality seems to be metastable, *i.e.* the macroscopic biaxiality disappears after removal of the alignment field.[15,21] Though it could not be excluded that also stable N_b phases might be possible, the presently proven cases of biaxial nematic phases seem to be only locally biaxial and the bulk biaxiality is induced under the experimental conditions (Fig. 1d and e).[11–13,15] This cluster model has direct consequences for symmetry considerations.[15] Accordingly, there is not only the case of highest orthorhombic symmetry (D_{2h}, Fig. 1b), but also lower symmetries could become possible, as for example C_{2h}, if the molecules are tilted with respect to a reference system provided by the cluster structure and if the rotation of the molecules around the long axis is restricted (Fig. 1c).[15]

Among the low molecular weight materials forming nematic phases, the bent-core mesogens[22] have received special attention, not only because of their potential to form biaxial[13,18,21,23–28] and ferroelectric nematic phases,[29b] but also as they show several other unusual properties, such as amplification of chirality,[30,31] huge flexoelectricity,[32,33] unusual electroconvection patterns[34,35] and special rheological properties,[35] which make them very distinct from usual nematic phases. However, there is still confusion about the nature of these bent-core nematic phases.

[a]*Organic Chemistry, Institute of Chemistry, Martin Luther University Halle-Wittenberg, Kurt Mothes Str. 2, D-06120 Halle (Saale), Germany. E-mail: carsten.tschierske@chemie.uni-halle.de; Fax: +49 345 552 7346; Tel: +49 345 552 5664*
[b]*Physical Chemistry, Institute of Chemistry, Martin Luther University Halle-Wittenberg, Von-Danckelmann-Platz 4, 06120 Halle (Saale), Germany*

† Electronic supplementary information (ESI) available: Synthesis and analytical data, additional crystallographic data and textures. See DOI: 10.1039/b923262a

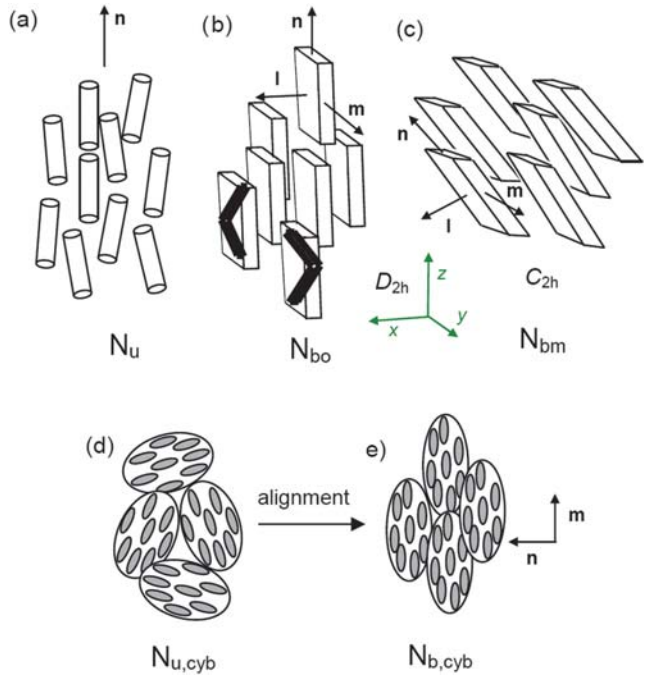

Fig. 1 Nematic phases of bent-core molecules: (a) unrestricted rotation around the molecular long axis **n** leads to an uniaxial nematic phase (N_u); (b) restricted rotation around **n**, but without polar order, leads to the simplest type of biaxial nematic phase (N_b) with orthorhombic D_{2h} symmetry (N_{bo} phase); (c) biaxial nematic phase with monoclinic C_{2h} symmetry (N_{bm} phase) as for example possible in the presence of a reference system provided by the organization of the molecules in SmC clusters with frozen rotation around **n**; if the direction of **m** would also deviate from the direction *y* (not shown) then the phase symmetry would be further reduced to triclinic (C_i, N_{bt} phase);[15] (d and e) clusters where the view is along direction *z* of the reference system; (d) rotationally disordered biaxial clusters, where the rotational disorder of the clusters around *z* leads to macroscopic uniaxiality; (e) phase biaxiality due to field- or surface-induced or spontaneous alignment of the biaxial clusters.

Whereas some authors have regarded them as nematic phases formed by orientationally ordered single molecules,[24,26] there are numerous indications that they actually represent cybotactic nematic phases,[29b,35–38] composed of small smectic clusters.[39,40]

Moreover, nematic phases are relatively rare among the mesophases of bent core molecules. The occurrence of nematic phases requires either molecules with extended aromatic cores and relatively short terminal chains, as provided by some *m*-terphenyls,[41] bent oligophenyleneethinylenes[23] and different types of naphthalene derivatives,[42] or a reduction of the molecular bent as provided by 5-membered heterocycles, like oxadiazoles (increased bending angle α),[13,18,19,25,26,28,29,31c,33,43,44] hockey stick molecules (having one short and one long leg)[45] and dimesogens composed of rod-like and bent units (average bent is reduced).[21,27,33,34c,46] However, in most cases these nematic phases occur above smectic or modulated smectic phases at relatively high temperatures (mostly >150 °C). For practical application nematic phases in wide temperature ranges around room temperature and without low temperature smectic or columnar phases would be required. Relatively low transition temperatures were indeed observed for resorcinol bisbenzoates with additional Cl, Br or CN substituents in 4-position of the bent resorcinol core

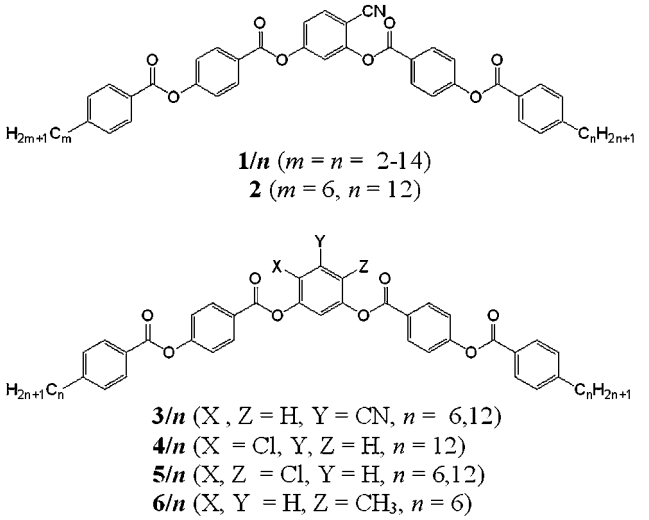

Chart 1 Structures of the bent-core mesogens under investigation.

which changes the molecular conformation by increasing the bending angle α to *ca.* 140°.[47] However, the existence of smectic phases below the nematic phases of these compounds and the observed field induced transformation to smectic phases are still disadvantageous.[31a,32,35,38,47–51]

This report provides new bent-core mesogens with broad nematic phase ranges, and some of them can be supercooled below room temperature without smectic low temperature phases. This was achieved in a homologous series of 4-cyanoresorcinol bisbenzoates (**1/*n***, see Chart 1) in which the alkoxy chains of previously known compounds[48] were replaced by alkyl chains. Secondly, a systematic investigation of the structure of the nematic phases depending on chain length and temperature is provided. It indicates a chain length dependent structural transition from nematic phases based on single molecules with only nearest neighbour interactions (N) for short chain derivatives to cybotactic nematic phases composed of relatively large clusters (N_{cybC}) for compounds with long chains. Moreover, there is also a strong temperature dependence of the cluster size. The knowledge about the organization in these nematic phases allows a deeper understanding of some special properties of the bent-core nematics and it provides a basis for future materials design, possibly leading to induced and even spontaneous biaxial nematic phases. Finally, the transition from nematic to smectic phases was investigated; this takes place in a sequence of at least two subsequent steps *via* an intermediate phase composed of locally connected, but not completely fused strings of cybotactic clusters (CybC).

2. Experimental

2.1. Synthesis

The target molecules **1/*n*** (see Chart 1) have been synthesized from 4-cyanoresorcinol and 4-(4-*n*-alkylbenzoyloxy)benzoic acids[52] by an acylation reaction using the carbodiimide method (Scheme 1).[53] 4-Cyanoresorcinol was prepared from commercially available 2,4-dihydroxybenzaldehyde by formation of the oxime followed by dehydration following a procedure described in the literature.[54] The 4-(4-*n*-alkylbenzoyloxy)benzoic acids[52]

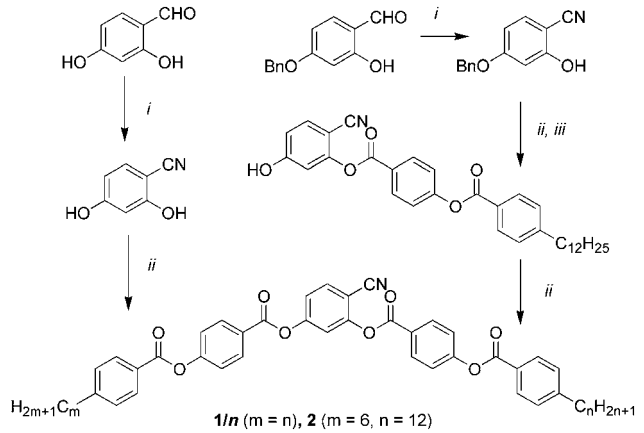

Scheme 1 Synthesis of compounds **1/n** and **2**. *Reagents*: (i) 1. H_2NOH, 2. Ac_2O, 3. NaOH; (ii) 4-(4-*n*-alkylbenzoyloxy)benzoic acid, DCC, DMAP; (iii) H_2/Pd/C.

were prepared starting from 4-*n*-alkylbenzoic acids by esterification with 4-hydroxybenzaldehyde followed by oxidation using sodium chlorite as oxidizing agent.[55] The isomeric 5-cyano substituted compound **3/*n*** as well as the chloro substituted derivatives **4/*n*** and **5/*n*** and the methyl substituted compound **6/6** (see Table 2) were prepared by esterification of 4-(4-*n*-alkylbenzoyloxy)benzoic acids with 5-cyanoresorcinol, 4-chlororesorcinol, 4,6-dichlororesorcinol and 4-methylresorcinol, respectively. The synthesis of compound **2**, incorporating two different alkyl chains, starts from 4-benzyloxy-2-hydroxybenzaldehyde. The free 2-OH group was first acylated with 4-(4-*n*-dodecylbenzoyloxy)benzoic acid and after hydrogenolytic debenzylation the 4-OH group was acylated with 4-(4-*n*-hexylbenzoyloxy)benzoic acid. Purification of all final compounds was carried out by column chromatography and crystallization from mixtures of *n*-hexane or ethanol with small amounts of dichloromethane. Experimental details and analytical data are reported in the ESI†.

2.2. Investigations

Phase transitions were determined by polarizing optical microscopy (Optiphot 2, Nikon) in conjunction with a heating stage (FP 82 HT, Mettler) and by differential scanning calorimetry (DSC-7, Perkin Elmer). The assignment of the mesophases was made on the basis of optical textures and by X-ray diffraction (XRD). Investigations on oriented samples were performed using a 2D detector (HI-Star, Siemens AG). Uniform orientation was achieved by alignment in a magnetic field ($B \approx 1$ T) using thin capillaries. This orientation is maintained by slow cooling (0.1 K min^{-1}) in the presence of the magnetic field. Electro-optical experiments have been carried out using a home built electro-optical setup in commercially available ITO coated glass cells (E.H.C., Japan) with a gap of 6 μm and a measuring area of 1 cm^2.

3. Results and discussion

3.1. Effects of structural variations on LC phases of bent-core mesogens

The phase transition temperatures, transition enthalpies and phase sequences of the 4-cyanosubstituted compounds **1/*n*** and **2** are summarized in Table 1. Upon cooling compounds **1/*n*** and **2**

Table 1 Transition temperatures (*T*/°C) and associated enthalpy values (in square brackets, ΔH/kJ mol^{-1}) of the 4-cyanoresorcinol bisbenzoates **1/*n*** and **2**[a]

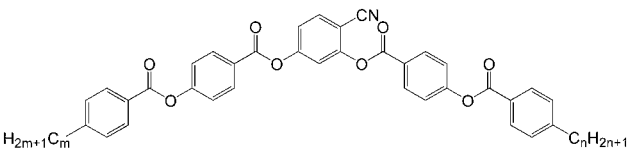

Comp.	*m*/*n*	Phase transitions					
1/2	2/2	Cr 127 [38.1]				(N 123 [0.4])	Iso
1/3	3/3	Cr 104 [48.9]				N 118 [0.4]	Iso
1/4	4/4	Cr 117 [38.4]				(N 107 [0.5])	Iso
1/5	5/5	Cr 108 [39.6]				N[b] 108.5 [0.5]	Iso
1/6	6/6	Cr 98 [37.1]				N_{cybC} 101 [0.5]	Iso
1/7	7/7	Cr 96 [35.5]		($SmC_{(I)}$ 25 [0.3]	CybC 41 [0.2])	N_{cybC} 111 [0.7]	Iso
1/8	8/8	Cr 98 [32.8]		($SmC_{(I)}$ 36 [0.8]	CybC 43 [0.3])	N_{cybC} 99 [0.7]	Iso
1/9	9/9	Cr 98 [35.1]		($SmC_{(I)}$ 50 [0.6]	CybC 58 [0.3])	N_{cybC} 104 [0.8]	Iso
2	6/12	Cr 86 [34.4]		($SmC_{(I)}$ 43 [0.3]	CybC 59 [0.2])	N_{cybC} 103 [0.8]	Iso
1/10	10/10	Cr 96 [30.2]	($SmC_{(II)}$ 58 [1.0]	$SmC_{(I)}$ 67 [0.1]	CybC 86 [0.1])	N_{cybC} 106 [1.4]	Iso
1/11	11/11	Cr_1 53 [12.7] Cr_2 91 [35.9]	($SmC_{(II)}$ 63 [0.6]	$SmC_{(I)}$ 68 [0.3])	CybC 94 [0.1]	N_{cybC} 107 [1.9]	Iso
1/12	12/12	Cr_1 86 [33.1] Cr_2 93 [13.2]		($SmC_{(I)}$ 70 [0.9])	CybC 103 [0.3]	N_{cybC} 111 [2.5]	Iso
1/14	14/14	Cr 91 [50.9] (M 36 [1.0]	$SmC_{(II)}$ 73 [0.6]	$SmC_{(I)}$ 77 [0.2])	CybC 114	N_{cybC} 115 [5.2][c]	Iso

[a] Peak temperatures in the first DSC heating curves (10 K min^{-1}), monotropic transitions (enclosed by round brackets) were taken from the second heating run. Abbreviations: Cr = crystalline solid (Cr_1 and Cr_2 represent different crystalline modifications); Iso = isotropic liquid; N = nematic phase with nearest neighbour correlation, similar to ordinary nematic phases; N_{cybC} = nematic phase composed of SmC type cybotactic clusters; CybC = mesophase composed of elongated cybotactic clusters; $SmC_{(I)}$ = synclinic tilted smectic C phase; $SmC_{(II)}$ = synclinic smectic C phase with enhanced packing density compared to $SmC_{(I)}$; all SmC-type phases do not show ferroelectric or antiferroelectric switching; M = mesophase with unknown structure; detailed X-ray data are collated in the ESI (Fig. S1–S18 and Tables S1–S11). [b] Assignment to N or N_{cybC} is for **1/5** not yet possible. [c] Phase transitions not resolved.

from the isotropic liquid state a schlieren texture with π/2 and π/4 disclinations and marbled domains occurs. The materials are highly fluid and the observed textural features are typical for nematic mesophases. With exception of the shortest even numbered homologues **1/2** and **1/4** which have monotropic (metastable) nematic phases, all other compounds **1/*n*** and **2** show enantiotropic phases. The nematic phases of compounds **1/3–1/6** with short chains can be supercooled to 20 °C without transition to another LC phase or crystallization (see Fig. 2a for a representative DSC curve). Crystallization sets in only after storage for several hours at room temperature or upon heating to *ca.* 50 °C. Compounds **1/7–1/14** and **2** with longer terminal chains show additional phase transitions, leading to mesophases composed of larger ribbon-like aggregates (CybC) and tilted smectic phases (SmC, see Fig. 2b). In the whole mesomorphic temperature range no polar (ferroelectric or antiferroelectric) switching can be observed. This is in contrast to related alkoxy substituted analogues where polar switching phases were observed below nonpolar SmC phases.[48] In the series of compounds **1/n** the N-Iso transition temperatures first strongly decrease with growing alkyl chain length and than increase again (Table 1). For compounds with a medium chain length (**1/5–1/9**) there is a pronounced odd–even effect with higher transition temperatures for the compounds with an odd number of C atoms in each alkyl chain.[56]

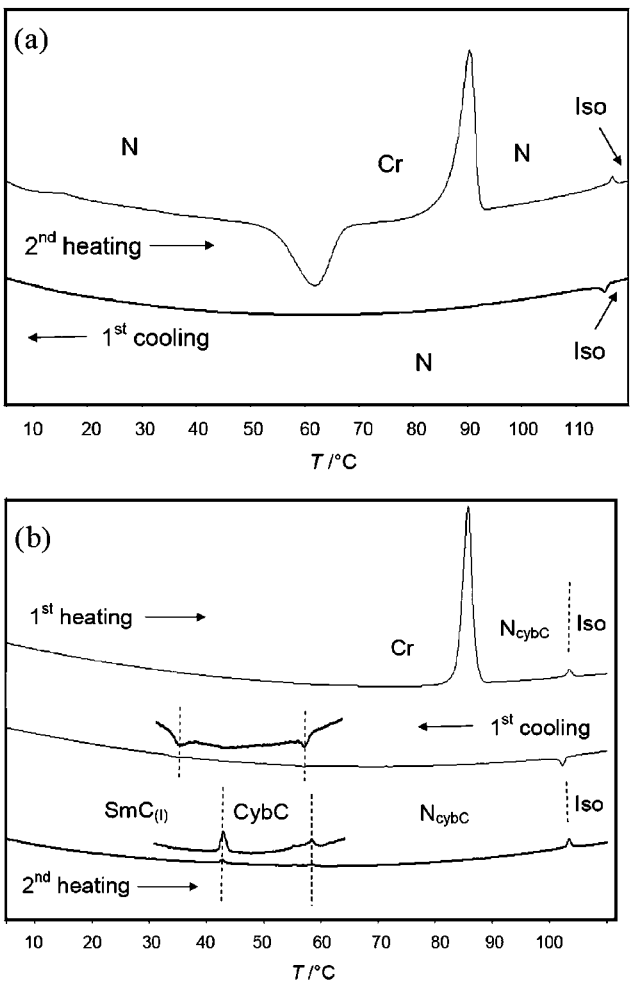

Fig. 2 Representative examples of DSC heating and cooling curves (10 K min^{-1}): (a) compound **1/3** as an example of a compound with an ordinary N phase, which can be supercooled below RT without crystallization; (b) compound **2** as an example for a compound showing a $SmC_{(I)}$–CybC–N_{cybC} trimorphism.

However, the scope of this approach (replacing alkoxy by alkyl groups) is limited and apparently restricted to the 4-cyano substituted resorcinol derivatives, whereas replacing alkoxy chains by alkyl chains in all other investigated cases leads only to a reduction of the mesophase stability or to a complete loss of LC phases without reducing melting points or crystallization tendency (see Table 2). For example, no nematic phases could be observed for the 5-cyanoresorcinol, 4-chloro and 4,6-dichlororesorcinol bisbenzoates **3/*n*–5/*n***. The 4-methyl resorcinol derivative **6/6** shows only a B1 type rectangular columnar phase, which was assigned by the very typical texture (Fig. S19†). This indicates that not only the size of the 4-substituent at the bent unit, but also its polarity contributes to formation of nematic phases by bent-core mesogens (compare CH_3 and CN which have a nearly identical volume of *ca.* 31 Å^3). Hence, the 4-substituent at the bent resorcinol unit seems to be not only responsible for opening the bending angle due to steric effects,[38,47–50] but also dipolar interactions between these lateral substituents appear to be important.

3.2. Structural transformations in the nematic phases

3.2.1 XRD investigations of magnetically aligned samples. X-Ray diffraction was carried out with the nematic phases of compounds **1/2**, **1/4**, **1/6–1/14** and **2**, oriented in a magnetic field with medium strength ($B \approx 1$ T, cooling rate 0.1 K min^{-1}, see Fig. S1–S18 and Tables S1–S11†). The diffraction pattern of compound **1/6** is shown in Fig. 3a and b as example. Diffuse wide angle maxima at $d = 0.47$ nm, corresponding to the mean lateral distance between the molecules, are centered on the equator indicating a fluid LC phase. The diffuse small angle scattering

Table 2 Transition temperatures of compounds **3/*n*–6/*n***[a]

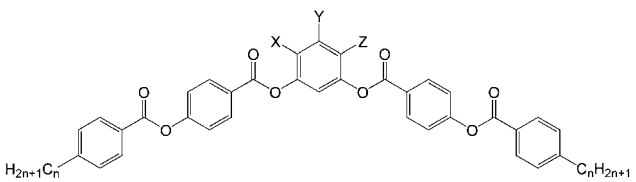

Comp.	*n*	X	Y	Z	T_m/°C	T_{cr}/°C
3/6	6	H	CN	H	117	103
3/12	12	H	CN	H	123	108
4/12	12	Cl	H	H	95	73 (M 60)[b]
5/6	6	Cl	H	Cl	101	79
5/12	12	Cl	H	Cl	93	85
6/6	6	CH_3	H	H	88	59 (B1 < 20)[c]

[a] T_m = melting temperature; T_{cr} = crystallization temperature obtained from the DSC curves (heating and cooling rates 10 K min^{-1}). [b] The monotropic mesophase M is a smectic or modulated smectic phase with a $T_{Iso–M}$ transition at 60 °C, but no nematic phase, a more detailed investigation was not possible due to rapid crystallization. [c] B1 phase with a $T_{Iso–B1}$ transition at 59 °C and crystallization below 20°C, phase assignment is based on the typical texture (see ESI Fig. S19).

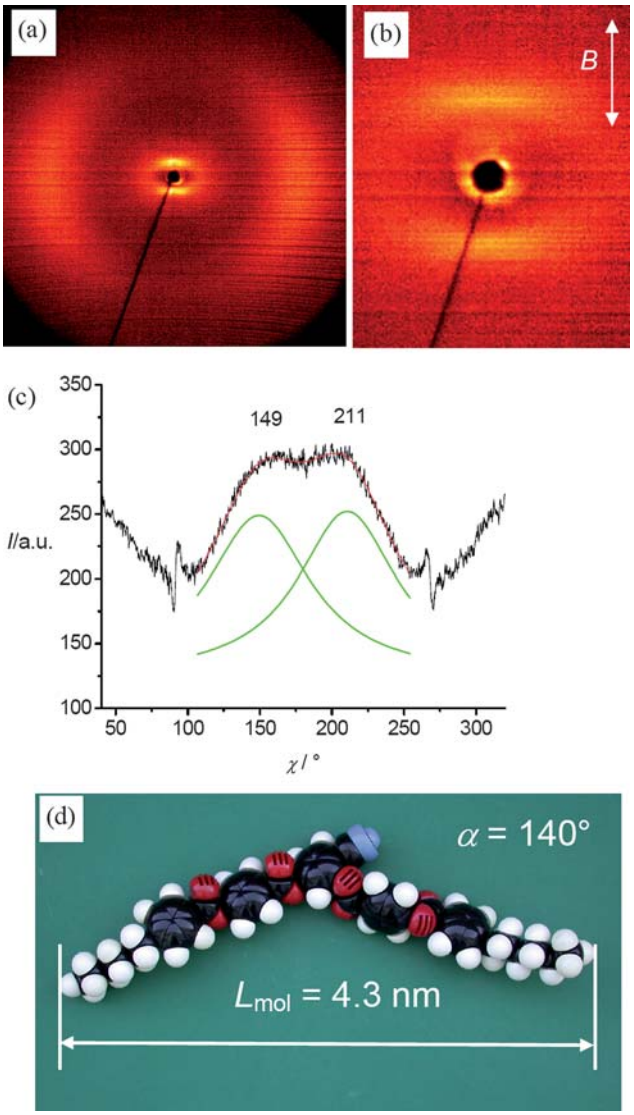

Fig. 3 Investigation of compound **1/6**: (a and b) X-ray diffraction pattern (wide angle and small angle) of a magnetically aligned sample at $T = 80$ °C; arrow indicates the direction of the magnetic field; (c) χ-scan over the diffuse small angle scattering, indicating the presence of SmC type cybotactic clusters, for additional information see Fig. S4 and S5†; (d) CPK model showing compound **1/6** in a V-shaped conformation with a bending angle $\alpha = 140°$ and stretched alkyl chains.

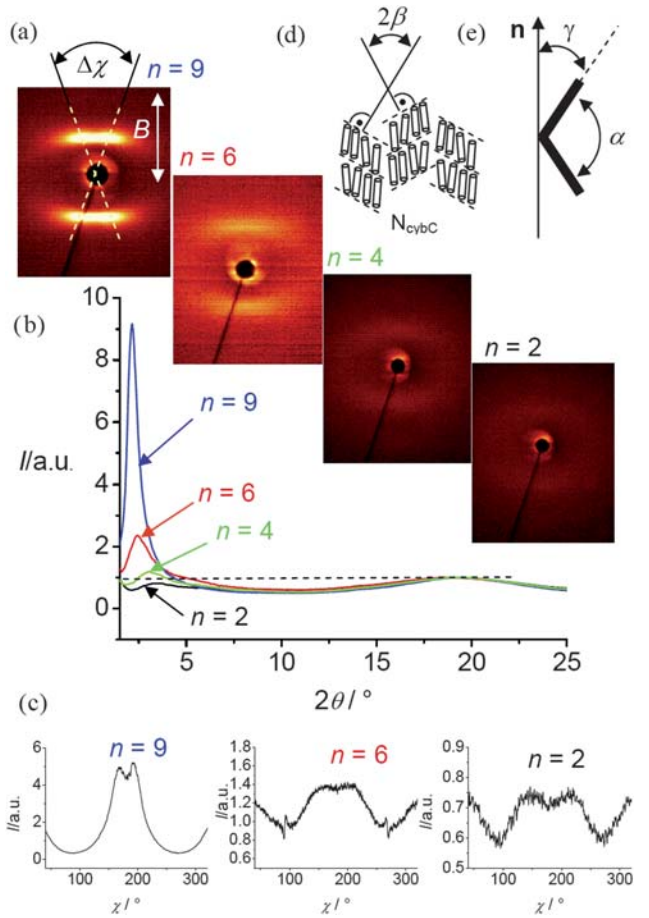

Fig. 4 (a) Small angle diffraction patterns of magnetically aligned samples (direction of the magnetic field is shown as white arrow) in the nematic phases of compounds **1/9** (65 °C), **1/6** (90 °C), **1/4** (90 °C) and **1/2** (105 °C), from top left to right bottom; (b) θ-scans over the small and wide angle scatterings (normalized to $I = 1$ for the maximum of the wide angle scattering) for **1/9** (90 °C), **1/6** (90 °C), **1/4** (90 °C) and **1/2** (105 °C); (c) χ-scans over the small angle regions for **1/9** (65 °C), **1/6** (90 °C) and **1/2** (105 °C); (d) organization of the molecules in a skewed cybotactic nematic phase (N_{cybC} phase) aligned under a magnetic field B parallel to the molecular long axis (rotationally disordered molecules) and (e) alignment of a single bent-core mesogen in a nematic field and definition of the molecular parameters.

has its maximum between $d = 3.71$ nm ($T = 60$ °C) and $d = 3.56$ nm ($T = 90$ °C) which is quite a bit smaller than the molecular length $L_{mol} = 4.3$ nm of **1/6** in a V-shaped conformation with a bending angle of 140°[57] and stretched alkyl chains in all-*trans* conformation (see Fig. 3d).

The intensity of the small angle scattering rises strongly with increasing chain length, as shown in the comparison in Fig. 4a and b for the nematic phases of compounds **1/2**, **1/4**, **1/6** and **1/9**. The small angle scattering of compounds **1/2** and **1/4** with the shortest chains is similar to that observed for ordinary nematic phases in which it has a lower or nearly equal intensity compared to the wide angle scattering ($I_s \leq I_w$). For compounds **1/6** and **1/9** with longer chains the intensity of the small angle scattering is much stronger than the wide angle scattering which, according to DeVries, indicates "cybotactic" nematic phases ($I_s \gg I_w$).[36] Cybotactic nematic phases, which are composed of small smectic clusters, can occur as pretransitional phenomena at the N–Sm transition,[58] but for nematic phases of bent-core mesogens the cybotactic structure typically presents an intrinsic phase structure over a broad temperature range (see below).

For the long chain compounds **1/9–1/14** the diffuse small angle scattering has clear maxima beside the meridian (dumbbell shape as shown in Fig. 4a for $n = 9$). The maxima are smeared out to streaks parallel to the equator for compounds with medium chain lengths (**1/6–1/8**), whereas for the short chain compounds **1/2–1/4** the shape of the small angle scattering is distinct, more crescent like and the intensity is much lower (see Fig. 4a, $n = 2$ and 4). Also in this case the χ-scans over the small angle regions clearly indicate four symmetrically located diffuse maxima (see Fig. 4c). The splitting of these maxima (plotted as $\Delta\chi/2$ against

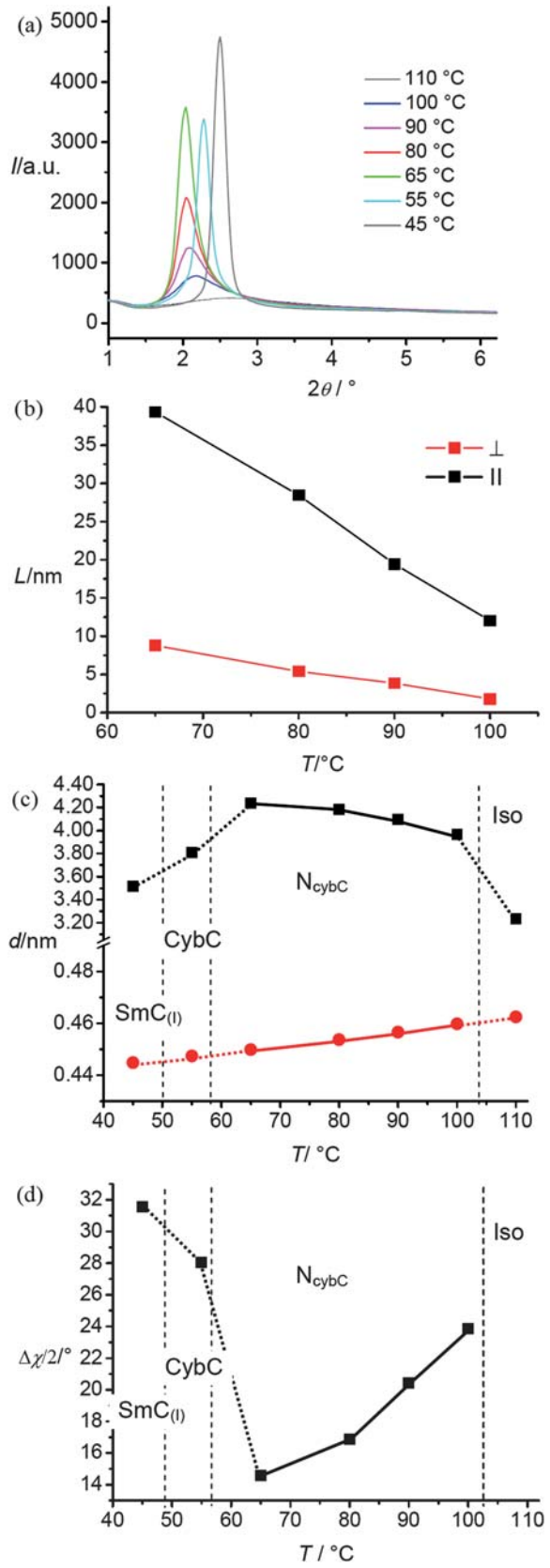

Fig. 5 Data of compound **1/9**: (a) θ-scans over the diffuse small angle scattering at various temperatures: 110 °C: Iso; 100, 90, 80, 65 °C: N_{cybC}; (b) longitudinal ($L_{\|}$) and transversal cluster size ($L_{\perp}$) as estimated from the full width at half maximum of the small angle scattering according to $3(\xi = 2/\Delta q)$ plotted against temperature; (c) temperature dependence of d-values corresponding to the maxima of the small angle scattering (filled squares) and the wide angle scattering (filled circles) and (d) temperature dependence of the splitting of the maxima of the diffuse small angle scattering in 2D XRD patterns of an aligned sample.

T in Fig. 6b and 7a) is the largest for compounds **1/2** and **1/4** ($\Delta\chi/2$ = 35–38°), then it steeply decreases to *ca.* $\Delta\chi/2$ = 15° for compound **1/10** and remains nearly constant upon further chain elongation (see Fig. 6b). For the short chain compounds **1/2–1/4** there is no significant change of shape, intensity and position of the small angle scattering with temperature (see Fig. S1–S3†), whereas for compounds **1/6–1/9** with medium chain length there is a strong temperature dependence (see Fig. 5a and d). For compounds with even longer chains the intensity of the small angle scattering is very strong and the nematic temperature range is only small, and therefore it is difficult to investigate the temperature dependence for these compounds in detail.

As shown in Fig. 5a for compound **1/9**, as an example, in the temperature range of the nematic phases between 65 and 100 °C the intensity of the small angle scattering strongly rises and the peak becomes sharper with decreasing temperature, whereas the wide angle scattering does not change significantly (Fig. S9b†). From the analysis of the small angle scattering the cluster size was estimated in longitudinal and transversal direction by measuring the intensity profiles of the peaks separately for the X and Y direction. The peaks were fitted to Lorentzian curves and the correlation length was estimated according to $\xi_{\|,\perp} = 2/\Delta q$ from the full width at half maximum (FWHM, Δq, see Table S6†) of the fitted curves.[59] The dimensions of the cybotactic clusters in longitudinal ($L_{\|}$) and transversal ($L_{\perp}$) direction, can be approximated to three times the correlation lengths $\xi_{\|}$ and $\xi_{\perp}$ respectively.[37] The same cluster size was obtained using the Scherrer eqn (1) assuming $K = 1$ (see Fig. S9c†).[60]

$$L_{\|,\perp} = K\frac{\lambda}{\Delta(2\theta)_{\|,\perp}\cos\theta_B} \quad (1)$$

The cluster size depends strongly on the length of the terminal alkyl chains. As shown in Fig. 6a for the short-chain compounds **1/2** and **1/4**, the calculated longitudinal cluster size $L_{\|}$ is only 1–3 nm, *i.e.* less than the molecular length (L_{mol} = 3.5–3.9 nm) and the transversal size $L_{\perp}$ is 1–1.5 nm, corresponding to 2–3 molecules arranged side-by-side. Hence, these nematic phases are similar to ordinary nematic phases with only short range correlation between nearest neighbouring molecules. On elongation of the alkyl chains the cluster size increases significantly up to values of $L_{\|}$ = 22 nm (5 molecules) and $L_{\perp}$ = 5 nm (10–11 molecules) for compound **1/10** (all values *ca.* 10 K below the nematic-to-isotropic transition). Even larger cluster sizes could be expected for the nematic phases of compounds **1/11–1/14**.[61] These nematic phases can be considered as cybotactic nematic phases composed of small SmC-like clusters.

As shown in Fig. 5b (see also Table S6†), the SmC clusters in the nematic phase of compound **1/9** continuously grow with decreasing temperature with a nearly linear dependence $L_{\|,\perp} = f(1/T)$ (Arrhenius behaviour, see Fig. S9d†). The longitudinal dimension $L_{\|}$ increases from 12 nm at T = 100 °C to 39 nm at T = 65 °C.[37] This means that at 100 °C the clusters are composed of

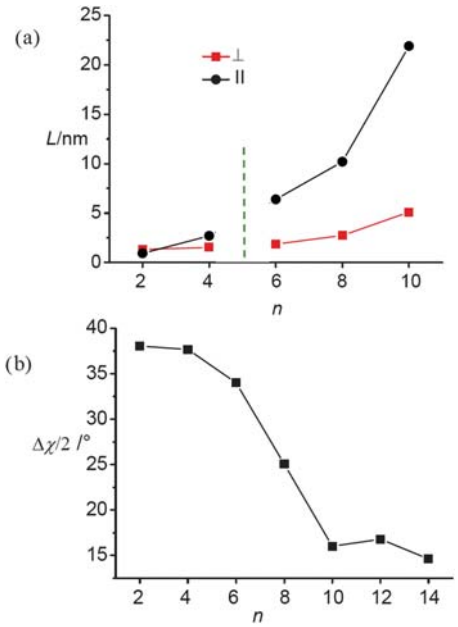

Fig. 6 (a) Longitudinal and transversal cluster size $L_{\parallel/\perp}$ and (b) splitting of the small angle diffraction maxima $\Delta\chi/2$ of compounds **1/*n*** depending on chain length, as determined for compounds **1/2**–**1/10** at T approximately 10 K below the transition to the isotropic (**1/2**: 115 °C; **1/4**: 100 °C; **1/6**: 80 °C; **1/8**: 90 °C; **1/10**: 100 °C; for compounds **1/12** and **1/14** with smaller nematic ranges data at 106 and 115 °C, respectively, are shown).

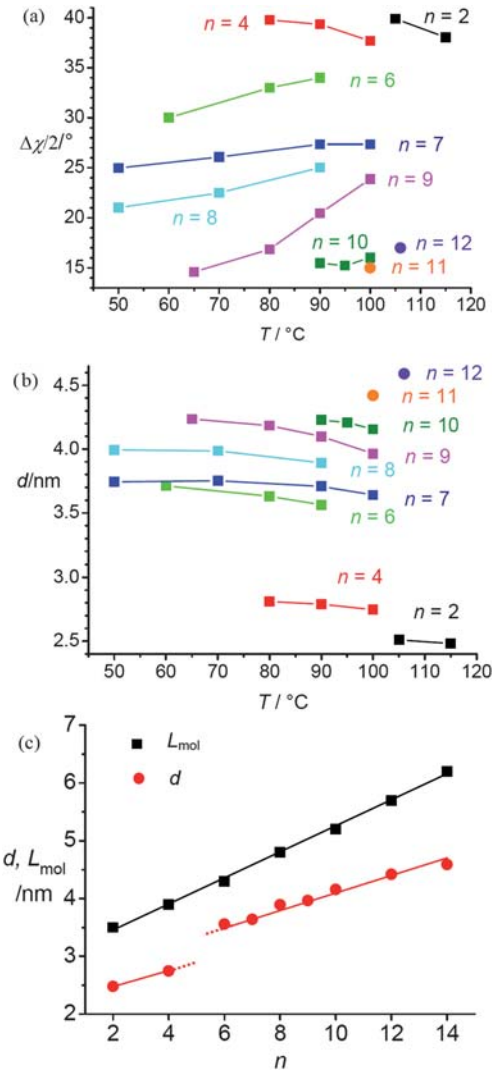

Fig. 7 Comparison of the XRD data of compounds **1/*n*** depending on chain length (n) and temperature: (a) small angle splittings $\Delta\chi/2$, (b) d-values; (c) plots of the calculated molecular length (L_{mol}, assumed bending angle 140°, all-*trans* alkyl chains, conformation as shown in Fig. 3d, see also Table S12†), and d-values at the highest measured temperature (see b).

about two to three layers and at 65° of about 8 layers of molecules (L_{mol} = 5.0 nm in a V-shaped conformation with 140° bending angle[57]). In the same temperature range the transversal dimension $L_\perp$ increases from 2 to 9 nm which corresponds to an increase from 4 to 18 molecules organized side-by side, assuming an average lateral molecular distance of approximately 0.46 nm (=maximum of the diffuse wide angle scattering, see Table S6†).[62,63] As the longitudinal size is obviously larger than the transversal size the clusters should have a prolate overall shape.

The increase of cluster size with decreasing temperature is associated with a steep decrease of the angle $\Delta\chi$, separating the maxima of the small angle scattering (given as $\Delta\chi/2$ values), from $\Delta\chi/2 = 24°$ at $T = 100$ °C to about 15° at $T = 65$ °C (Fig. 5d). In a similar manner also the growing cluster size with increasing chain length is associated with a decrease of the angular splitting from $\Delta\chi/2 = 38°$ for **1/2** to about 15° for **1/10**. The nematic phases of compounds **1/12** and **1/14**, forming large cybotactic clusters have nearly identical splitting around $\Delta\chi/2 = 15$–18° (see Fig. 6b).

Here, it must at first be considered that the $\Delta\chi$ splitting of the small angle scattering, if it would be interpreted as resulting from a tilt, would present the average tilt of aromatic and aliphatic segments. Because the alkyl chains are more disordered than the bent aromatic cores, with increasing alkyl chain length the $\Delta\chi$ splitting should decrease. However, in the series **1/*n*** the decrease in $\Delta\chi$ splitting is much larger than expected for the change of the bent-core-to-chain length ratio and there is no linear dependence of the $\Delta\chi$ splitting on chain length (Fig. 6b) as would be expected in this case. Hence, there should be other reasons contributing to the observed strong chain length dependence of the small angle splitting. Fig. 7a shows the $\Delta\chi$ splitting ($\Delta\chi/2$) of all investigated compounds **1/*n*** depending on temperature and chain length. It indicates that only for the short chain compounds **1/2** and **1/4** $\Delta\chi$ increases with decreasing temperature, whereas for all compounds with longer chains $\Delta\chi$ decreases. Hence, there is a distinct behaviour of the short chain compounds **1/2** and **1/4** and the long chain compounds **1/6**–**1/10** and there seems to be a relation between cluster size and the small angle splitting $\Delta\chi$. Despite the distinct temperature dependence of $\Delta\chi$, an increase of the d-value with decreasing temperature is observed for all compounds **1/*n*** (Fig. 6b). It is also remarkable that there is a distinct jump in d-spacing between compound **1/4** and **1/6**, again indicating a difference between short chain compounds and those with $n \geq 6$ (Fig. 7b).

Concerning the origin of the small angle splitting in the nematic phases of bent-core molecules there are presently two different explanations. (i) The dumbbell shape of the splitting

observed for the long chain compounds is the same as usually observed for skewed cybotactic nematic phases of rod-like molecules,[36] aligned under a magnetic field. As the long molecular axis (director **n**) is aligned parallel to the magnetic field the diffuse wide angle scattering (mean distance between the aromatic cores and between the alkyl chains) is centered on the equator (Fig. 3a) whereas the small angle scattering splits due to the skewed arrangement of the SmC clusters (Fig. 3b and 4a and c). This kind of diffraction pattern was recently simulated by Vaupotic *et al.* for molecules with bent aromatic cores, separated by alkyl chains with reduced electron density and assuming a core length corresponding to half of the total molecular length. In these calculations it was also considered that the molecules are organized in SmC clusters with longitudinal and transversal correlation lengths of 10 molecules. These simulations have shown that the small angle splitting indeed originates mainly from the structure factor, *i.e.* from the tilted organization of the bent-core mesogens in the smectic C type clusters.[64] (ii) On the other hand, Acharya *et al.* and Kumar *et al.*[24,26] assumed that the nematic phases do not have a cybotactic cluster structure. These authors calculated the XRD patterns for a nematic phase formed by densely packed individual bent-core molecules with only nearest neighbour interaction and did not consider the longitudinal electron density modulation caused by the terminal alkyl chains. These calculations also indicate a splitting of the small angle scattering, but in this case the splitting was attributed to the distinct tilt directions of the two rod-like wings forming the bent aromatic cores (see Fig. 4e).[24,26] These calculations gave a splitting of the maxima of the small angle scattering by $\Delta\chi = 80°$ for 1,3,4-oxadiazoles[13b] with a bending angle of $\alpha = 140°$. Interestingly, according to NMR studies,[47] the bending angle of compounds **1/*n*** is also about 140°, and the splitting of the small angle maxima of the short chain molecules **1/2** and **1/4** is in the range of $\Delta\chi = 70$–$80°$ ($\Delta\chi/2 = 35$–$40°$, see Fig. S1–S4†), *i.e.* close to the calculated splitting. Hence, it seems that the splitting of the small angle scattering of the short chain bent-core compounds **1/2** and **1/4** could indeed be due to the bent molecular structure as proposed by Acharya *et al.*[26] This is also in line with results obtained by Vaupotic *et al.*, showing that in this case the scattering intensity should be very weak[64] whereas it is high in the N_{cybC} phases (see Fig. 4a).

In contrast to the short chain compounds, for the long chain molecules **1/10–1/14**, forming N_{cybC} phases, the position of the relatively sharp and intense small angle reflections is mainly determined by the structure factor, *i.e.* by the tilted arrangement of the molecules in the SmC-type clusters. The tilt of the molecules in these cybotactic clusters is about 15–18° for the compounds investigated herein (Fig. 6b and 7a).

The situation is more difficult for molecules with a medium chain length (**1/6–1/9**). For these compounds, with increasing chain length, a continuous decrease of the small angle splitting (Fig. 6b) as well as an increase of the scattering intensity is observed (Fig. 4b), indicating a continuous growth of the cluster size with chain length. In addition, there is a significant temperature dependence. At high temperature these nematic phases have relatively small clusters and the clusters strongly grow with decreasing temperature (Fig. 5b). Hence, there is a chain-length and temperature dependent change of the contributions of the structure factor to the splitting and intensity of the small angle scatterings. A large splitting and low intensity is observed at high temperature and a smaller splitting with high intensity at lower temperature (Fig. 5d). Hence, for these medium-chain bent-core compounds the measured angular splitting of the small angle scattering ($\Delta\chi/2$) is neither directly related to the bending angle α nor to the tilt angle β of the molecules in the clusters (see Fig. 4d and e). Instead there is a complex relation between molecular structural features (form-factor), cluster size and tilt angle (structure factor) which determine the value of the experimentally measured angular splitting. This is important to note, as most of the previously investigated bent-core molecules forming nematic phases do actually fall into this category. The reason is that for this type of bent-core molecules the broadest ranges of the nematic phases can be achieved, whereas molecules with shorter chains easily crystallize and molecules with longer chains form predominately smectic phases.

Fig. 7c compares the experimentally observed *d*-spacings of the maxima of the diffuse small angle scattering with the calculated molecular lengths (assuming 140° bending angle in all cases). The main feature is a distinct jump upon transition from the N phases of compounds **1/2** and **1/4** ($d/L_{mol} = 0.71$) to the N_{cybC} phases of **1/6** ($d/L_{mol} = 0.83$) and longer compounds. This could be partly explained by an increase of the orientational order parameter at the transition from the nematic phases with only nearest neighbour interactions (average tilt resulting from the orientational order parameter is *ca.* 30°)[65] to the cybotactic nematic phases, because in the N_{cybC} phases the molecules are organized in smectic layer fragments where a much higher orientational order parameter is achieved. This leads to a reduction of the average tilt. As the tilt in the SmC clusters is only about 15–20° (*i.e.* smaller than the average tilt in the N phases) a shift of the small angle scattering maximum to larger *d*-values is observed in the N_{cyb} phases. The temperature dependence of the *d*-spacing (Fig. 7b) is in all cases in line with the increase of the orientational order parameter at reduced temperature.[66]

One point, which is not completely clear at present, is the fact that also in the N phases of the short chain compounds **1/2** and **1/4** the wide angle scattering is centered on the equator (see Fig. S1–S4†), though it is assumed that for these compounds the small angle splitting is caused by the distinct orientations of the rod-like wings. In this case, for samples aligned along the director **n** in a magnetic field, it would be expected that the wide angle scattering should split, too. Interestingly, also the preliminary simulation results reported by Acharya *et al.* show the wide angle scattering on the equator,[26b] which is in line with our experimental findings.

In summary, in the nematic phases of the series of compounds **1/*n***, depending on chain length and temperature, there is a structural transformation between distinct micro-structures. The N phases of compounds **1/2** and **1/4** with extremely short chains are more similar to ordinary nematic phases with only short-range correlation between the molecules. The nematic phases of the long chain compounds **1/10–1/14** are skewed cybotactic nematic phases composed of relative large clusters of layer stacks (N_{cybC}), *i.e.* these nematic phases can be rather regarded as strongly fragmented SmC phases with long range nematic order of clusters with local smectic order. In fact for these compounds the intensity of the small angle reflections does not change dramatically at the N_{cybC}-to-CybC-to-SmC

transition (see Fig. 5a), which is in line with this assumption. Also the transition enthalpy values of the N_{cybC}-to-CybC and CybC-to-SmC transitions are small (0.1–0.9 kJ mol^{-1}, see Fig. 2b and Table 1).

The fact that the splitting $\Delta\chi/2$ of **1/9** at low temperature ($\Delta\chi/2 = 15°$, see Fig. 5d) corresponds to the tilt observed in the N_{cybC} phases of the long chain compounds suggests that the actual tilt angle in the SmC clusters should be about 15–20° for all compounds **1/*n***, nearly independent on chain length and temperature. Compared with the smectic phases of bent-core molecules, which usually have tilt angles around 35°,[22] the tilt in the SmC clusters is relatively small. Here it must be considered that the layer fragments have a small size in the cybotactic N phase, and therefore, the chains can easily escape into the periphery forming aliphatic excrescences around the clusters. These aliphatic excrescences fit into the grooves at the periphery around the more dense packed aromatic regions of adjacent clusters. This steric fit provides a (non-regular) shift of the clusters with respect to each other. This inhibits the fusion of the cybotactic clusters and seems to be responsible for distortion of layer formation for bent-core mesogens, even if they have relatively long chains (*e.g.* **1/12** and **1/14**). This explanation is also in line with the observation that upon formation of smectic phases (by reducing temperature) the tilt angle increases. For example, for compound **1/9** the tilt rises from 15° in the nematic phase at 65 °C to about 32° in the SmC phase (see Fig. 5d). Because in the infinite layers of smectic phases the alkyl chains have no possibility to escape, a higher tilt is required at the transition to SmC to avoid layer frustration. It should also be noted that the line shape of the small angle scattering in the cybotactic nematic phases of compounds **1/*n*** can only be fitted to Lorentzian-type curves, which indicates that these are dynamic fluctuating system.[37,67]

As the SmC phases occurring below the nematic phase are non-polar phases (see Section 3.3) it is likely that also in the clusters there is no polar order or only a short range polar packing of the molecules, *i.e.* the bent-core molecules are on time and space average rotationally disordered around their long axes. Local biaxiality in the individual clusters would in this case result from the uniformly tilted organization of the molecules in the clusters (improper biaxiality), but a local C_{2h} type biaxiality or even local polar order cannot be completely ruled out at present. In any case the biaxiality of the SmC clusters is cancelled on a macroscopic scale due to the space and time averaging of the orientations of the clusters (see Fig. 1d). Therefore, these mesophases are optically uniaxial, but very easily show induced biaxiality due to alignment effects, as shown in Section 3.2.2.

For compounds with an intermediate chain length (**1/6–1/9**) a strong change of cluster size depending on temperature is found (see Fig. 7a). This means that for these compounds there is a continuous structural transition from a N-like nematic phase at higher temperature to a N_{cybC} nematic phase at lower temperature. This change of the cluster size leads to chain length dependent and temperature dependent changes of the properties of these nematic phases, manifested for example, in changes of the alignment behaviour as discussed in the following.

3.2.2 Textures and changes of alignment. Upon cooling from the isotropic liquid state the nematic phases appear with birefringent (yellow) Schlieren textures, indicating a predominately homogeneous alignment (director **n** on average parallel to the substrate surfaces). A characteristic feature of the long and medium chain compounds **1/*n*** and **2** is a strong increase of the birefringence immediately after the Iso-to-N transition which is shown in Fig. 8 for compound **1/10** as an example. Upon decreasing the temperature the texture rapidly changes the birefringence color (Fig. 8a–d), indicating a strong increase of the birefringence on cooling from 106 to 100 °C, most probably due to an increase of the order parameter as a result of the growth of the clusters. This change is continuous and reversible, but sometimes additional discontinuous and irreversible changes of the birefringence colour were also observed, as shown in Fig. 8e (change from green to orange). This non-continuous textural change is not associated with any enthalpy in the DSC curves or any change in the X-ray diffraction pattern (see Section 3.2.1) and it depends strongly on the experimental conditions. Therefore, it is not a phase transition, but rather realignment as a consequence of the growing cybotactic clusters with decreasing temperature and this is strongly dependent on the properties of the surface.[68] Moreover, often a slow transition to a homeotropic alignment takes place (dark areas in Fig. 8f) and after a certain period of time (few minutes) the whole sample can become uniformly dark. This spontaneous homeotropic alignment is often observed for the nematic phases of compounds **1/*n*** with

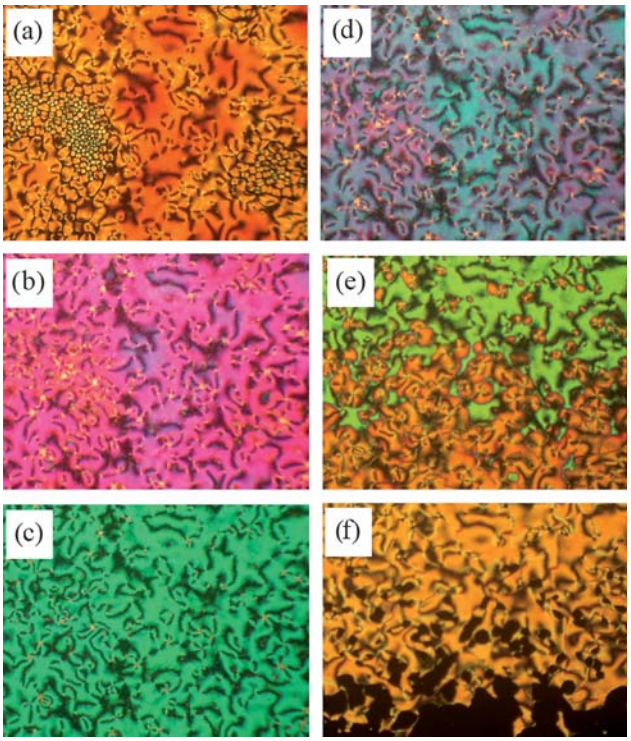

Fig. 8 Textures of compound **1/10** in the N_{cybC} phase (a–e) as seen between crossed polarizers (6 μm ITO cell, EHC, Japan): (a) Iso-to-N_{cybC} transition at $T = 106$ °C (nematic droplets and Schlieren texture; (b) N_{cybC} phase at $T = 105$ °C; (c) $T = 104$ °C; (d) $T = 103$ °C; (e) irreversible realignment in the N_{cybC} phase with change of the birefringence colour at around $T = 98$ °C; (f) slow irreversible realignment to homeotropic orientation at $T = 90$ °C (bottom, if sufficient time is given the complete area becomes dark).

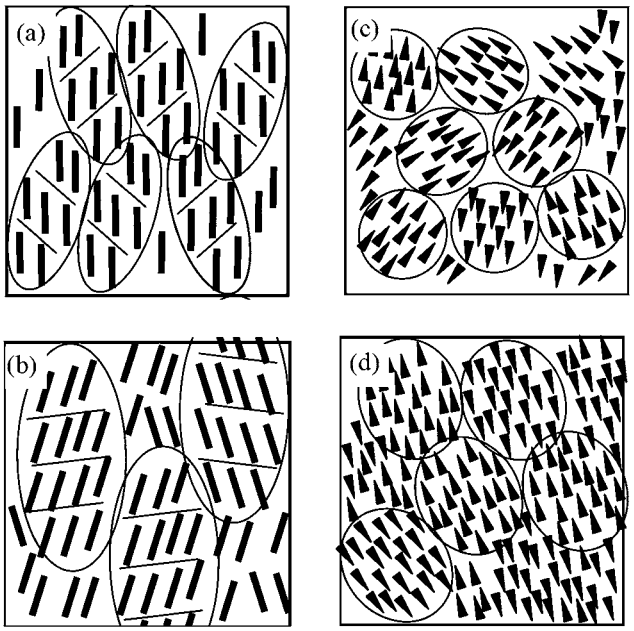

Fig. 9 Sketches showing the possible changes of the alignment of the cybotactic SmC clusters in the N_{cybC} phases (all views perpendicular to the surfaces of the cell): (a and b) homogeneous alignment with the molecules parallel to the surfaces (the bent-core molecules are assumed to be rotationally disordered around their long axes, hence molecular bent is neglected and the molecules are shown as straight lines); (a) for small clusters alignment is determined by the individual molecules; (b) larger clusters align with the cluster long axis; (c and d) homeotropic alignment, cybotactic clusters align with their layer planes parallel to the surfaces, the molecules are tilted with respect to the surfaces, arrows indicate the tilt direction of the molecules; (c) the clusters are orientationally disordered, leading to optical isotropy of the N_{cybC} phases; (d) alignment of the cybotactic clusters leading to biaxiality.

medium and long alkyl chains (**1/9–1/12**) upon approaching the transition to the non-nematic low temperature phases. Once formed, the homeotropic texture is stable up to the clearing temperature. All these textural transformations do not appear in the non-cybotactic N phases of compounds **1/2–1/4**.

Models showing a possible explanation for the observed textural changes in the nematic phases are sketched in Fig. 9a–c. Accordingly, at high temperature the clusters are small and alignment is mainly determined by the organization of the individual molecules with their long axes parallel to the surfaces and parallel to each other (planar alignment, Fig. 9a). With decreasing temperature, the size of the smectic clusters increases. It appears that these clusters become the dominating entities which align parallel to the surfaces and parallel to each other (Fig. 9b). This could explain the discontinuous texture changes associated with reduction of temperature as shown in Fig. 8e. After reaching a certain size, the clusters seem to prefer an orientation with their layer planes parallel to the substrate surfaces, leading to a homeotropic alignment (Fig. 9c).

Although the SmC clusters are intrinsically biaxial (most likely due to an improper biaxiality resulting from the tilt of the director **n**), on a macroscopic scale they are orientationally randomized, leading to a nearly optically isotropic appearance of these homeotropically aligned regions (see Fig. 8f), but

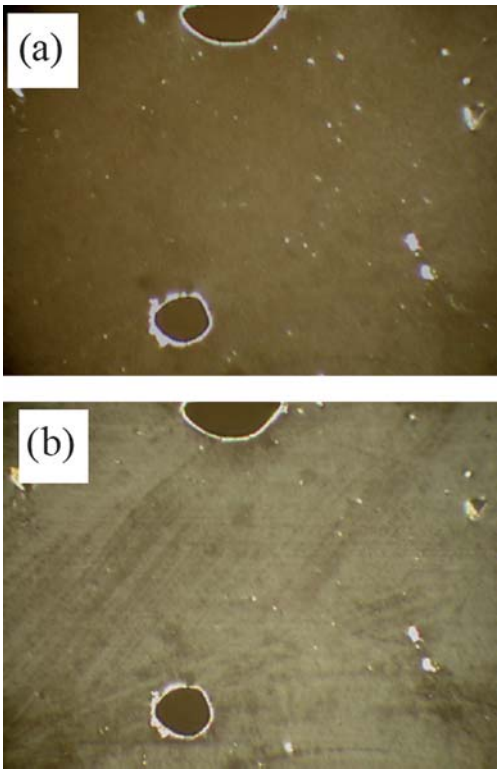

Fig. 10 Textures of the nematic (N_{cybC}) phase of **1/11** in a homeotropically aligned region between crossed polarizers: (a) weak birefringence at $T = 105$ °C; (b) increased birefringence at $T = 96$ °C.

nevertheless, a very weak birefringence is observed for medium and long chain compounds, as shown in Fig. 10a for the nematic phase of **1/11**. The birefringence continuously increases with decreasing temperature (Fig. 10b). This is most likely caused by a surface induced uniform alignment of the SmC clusters (Fig. 9d).[69] With decreasing temperature the surface anchoring becomes stronger and this enhances the birefringence.

3.2.3 Electro-optical investigations. As recently reported for other bent-core mesogens,[34c,d,70] also for the nematic phases of compounds **1/*n*** with $n = 2$, 4 and 6 a frequency dependent reversal of the dielectric anisotropy was observed. At high frequency (>5 kHz for **1/6**) the dielectric anisotropy is negative, leading to a highly birefringent homogeneous alignment characterized by the occurrence of strong hydrodynamic instabilities (see Fig. 11a). The dielectric anisotropy becomes positive at lower frequency (<1 kHz for **1/6**) and with increasing voltage the birefringence is reduced, leading to a dark homeotropically aligned area, indicating uniaxiality of the nematic phases of compounds **1/2–1/9** (Fig. 11b) due to the rotational disorder of the SmC clusters (see Fig. 1d). The frequency required for the transition from negative to positive dielectric anisotropy is shifted to lower frequencies with increasing chain length and for compound **1/10** the negative dielectric anisotropy is retained down to very low frequencies (and under an AC field). Hence, for long chain compounds **1/10–1/14** it was not possible to use this electric field induced alignment to check phase biaxiality. It is also interesting to note that for none of the investigated compounds **1/2–1/10** up to a voltage of 400 V (peak-to-peak, 6

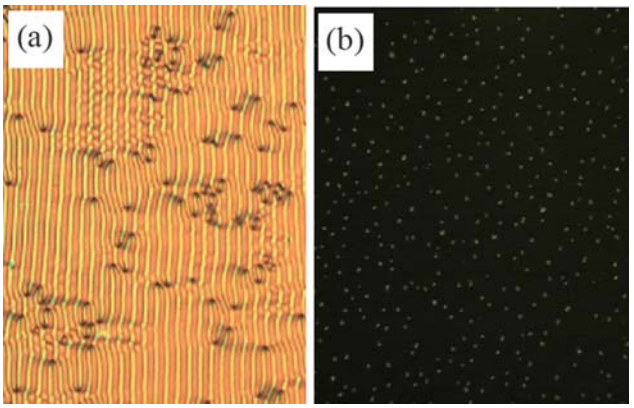

Fig. 11 (a) Electrohydrodynamic instabilities as seen for the nematic phase of compound **1/6** at $T = 60$ °C under a high frequency triangular wave electric field of 5 kHz (6 μm ITO cell), $U = 400$ V_{pp} (V_{pp} = peak-to-peak voltage); (b) homeotropic alignment as seen at low frequency (0.5 kHz at $T = 90$ °C; $U = 340$ V_{pp}), the small birefringent spots are defects.

μm cell) a smectic phase can be induced. This behaviour is distinct from related alkoxy substituted molecules in which a relatively low voltage of only *ca.* 10 V (6 μm cell) is sufficient to induce a SmC phase.[15,48] The reason for the distinct behaviour of the alkyl substituted compounds **1/*n*** compared to the related alkoxy substituted compounds might be the missing of a polar SmC phase ($SmCP_A$) in this series of compounds which could be due to the less densely packed organization of the alkyl substituted molecules, as discussed in more detail at the end of Section 3.3.2.

3.3. Tilted smectic and modulated smectic phases of compounds 1/*n*

3.3.1 Compounds 1/7–1/9 and 2 with medium chain length. As shown in the previous section for the cybotactic nematic phase of compound **1/9**, there is a continuous growth of the size of the cybotactic clusters with decreasing temperature (Fig. 5a and b and S9a†) which leads to an increase of intensity and sharpness of the small angle scattering. For compound **1/9** (and all other compounds with longer chains) there is a transition to a SmC phase which takes place as a multistep process. The changes of the textures at these transitions are shown in Fig. 12 at the right. This figure also shows the change of the X-ray diffraction pattern of a magnetically aligned sample of compound **1/9** depending on temperature.

The first phase transition at $T = 58$ °C is associated with a small transition enthalpy of only 0.3 kJ mol^{-1}, a distinct change of the textures, and the onset of phase biaxiality in the homeotropically aligned optical isotropic regions (Fig. 12b and c, right). At this transition the small angle scattering is split into two clear maxima. As the structure factor is dominating the XRD pattern of the N_{cybC} phases of the long chain compounds (see Section 3.2.1) and the LC phases are composed of larger aggregates (CybC) or layers (SmC), for these mesophases the splitting of the small angle scattering $\Delta\chi/2$ corresponds to the tilt angle β. Hence, in this case the change of $\Delta\chi/2$ at the phase transition indicates that the tilt angle is nearly doubled from 15° in the N_{cybC} phase to 28° in the new phase ($d = 3.81$ nm, see Fig. 12c). The intensity of all four small angle spots remains equal, indicating that an equal distribution of the tilt directions is retained. The sharpness of these reflections does not increase significantly at this phase transition and it is very similar to that in the cybotactic nematic phase close to this transition (Fig. 5a). It is also remarkable that the shape of these small angle scatterings changes from a more dumbbell-like shape aligned parallel to the equator in the N_{cybC} phase to an arrangement of the distinct scatterings more similar to a positioning on a ring around the primary beam, as typically observed for columnar or smectic phases. This indicates that the cybotactic clusters might fuse to elongated aggregates. In addition, two weak and relatively sharp reflections appear on the meridian (see arrows in Fig. 12c). The same observation was made for the shorter homologue **1/8** and for compound **2** with two distinct alkyl chains having in total the same length as compound **1/9** (Fig. S7 and S17†). For compound **2** beside the reflections on the meridian (with same θ-values as **1/9**) additional sharp reflections can be observed (see Fig. 13a and b). This pattern can be indexed to an oblique lattice with parameters $a = 6.51$ nm, $b = 7.77$ nm and $\gamma = 127.3°$. Remarkably, the remaining four strong and more diffuse scatterings are incommensurate with this 2D lattice, which can be explained either by a coexistence of this lattice with a phase composed of cybotactic clusters, or by a 2D lattice developing in a direction distinct from the direction of the layer periodicity in the clusters, effectively leading to a 3D structure. Because the viscosity of this phase is between that of the N_{cybC} phase at higher temperature and the SmC phase at lower temperature, and there are no extra reflections which can only be assigned to a 3D lattice, it is unlikely that a 3D lattice is formed. As the small angle scattering remains relatively diffuse it is thought that the cluster structure itself is retained, but the size of the clusters slightly increases, associated with a doubling of the tilt angle. It is likely that the SmC type clusters line up and fuse to elongated ribbon-like aggregates. The fusion in one direction restricts the chains packing and this might increase the tilt angle of the molecules. If a ribbon structure is assumed to be responsible for the occurrence of this 2D lattice (see Fig. 13c) the number of molecules organized in the diameter of each ribbon, as calculated from the number of molecules per unit cell (see ESI†, Section 1.11), is about 14. This value is close to the transversal correlation length found in the clusters of the adjacent N_{cybC} phase (about 18 molecules). Hence, at this phase transition the cybotactic clusters seem to fuse with formation of elongated aggregates composed of stacks of SmC-like ribbons. It appears that under the influence of the magnetic field[71] the SmC ribbons in adjacent clusters could organize on a long range oblique 2D-lattice (sharp spot pattern). However, in the majority of the sample where the alignment forces provided by the magnetic field are not sufficiently strong or distorted by competing forces (as for example surface effects) only short range positional order of the SmC ribbons occurs and hence a diffuse four-spot pattern is retained. The fact that the *d*-value of the diffuse scatterings is commensurate to ½ *b* of the Col_{ob} lattice is in line with this assumption (see Fig. 13c). This phase, which is formed as an intermediate structure at the N_{cybC}-to-SmC transition, is tentatively assigned as CybC standing for a phase based on elongated cybotactic clusters of the SmC type which is distinct from the cybotactic nematic phase (N_{cybC}) by a long range orientation correlation between the clusters leading to

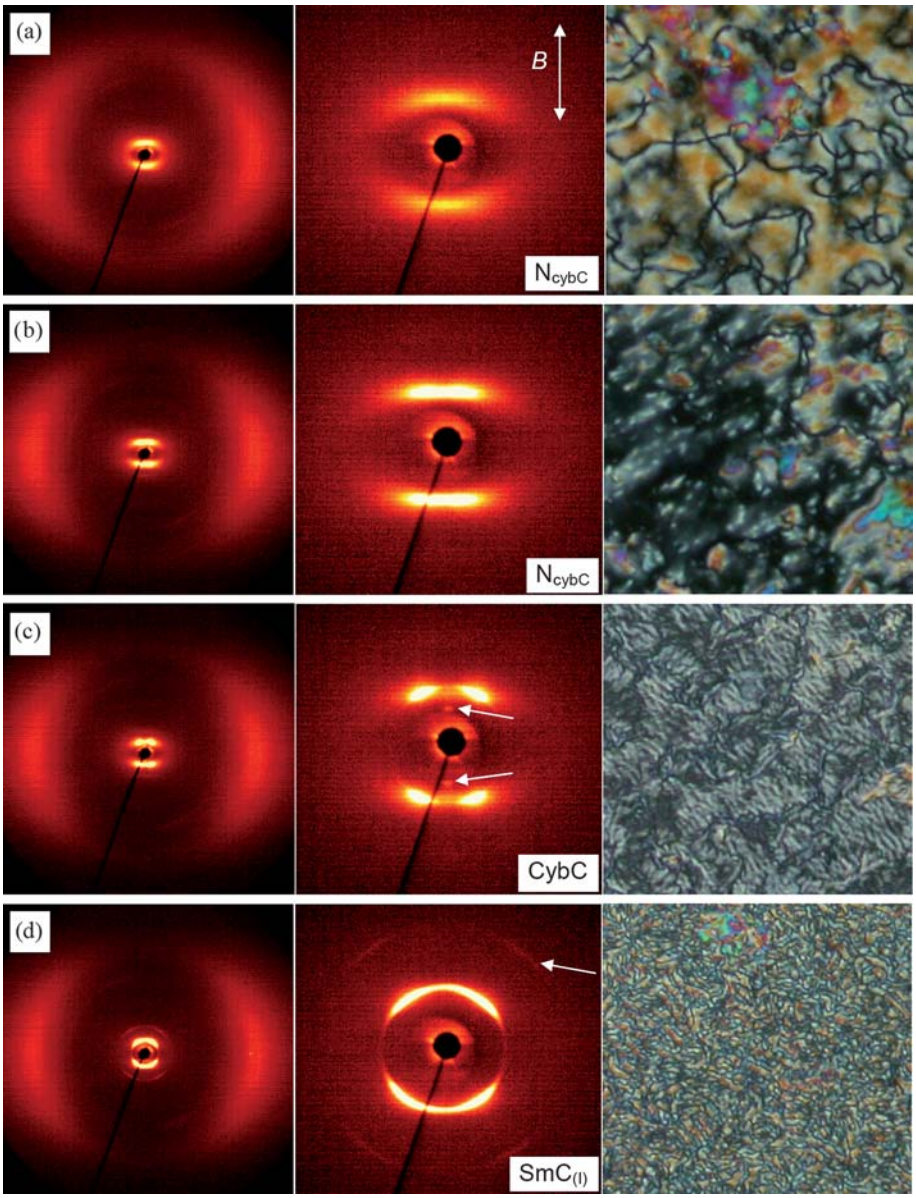

Fig. 12 X-Ray diffraction patterns (wide angle patterns at the left and small angle patterns in the middle) of a sample aligned in the magnetic field and textures as seen between crossed polarizers (at the right) of compound **1/9**: (a) N_{cybC} phase at 100 °C; (b) N_{cybC} phase at 65 °C; (c) CybC phase at 55 °C, arrows indicating additional sharp reflections on the meridian, and (d) $SmC_{(I)}$ phase at 45 °C, arrow indicating the second order layer reflections.

spontaneous macroscopic phase biaxiality. It is also distinct from a proper SmC phase as the clusters are not yet fused to quasi-infinite layers. Similar types of intermediate phases (assigned as X_1, X_2,[42d] N_x,[45a] and N_{col}[72]) were previously observed at the transitions from cybotactic nematic to columnar phases and B6 type phases[73] and were regarded as a special kind of columnar nematic phase where finite ribbons of smectic layers are arranged with long range orientational, but short range positional order.[74] The observation of a similar phase at the N_{cybC}-to-SmC transition indicates that the occurrence of such intermediate phases is a typical feature of the transitions from nematic to smectic and modulated smectic phases in bent-core mesogens.

In the case of compound **2** crystallization occurs on further cooling the CybC phase, whereas for compound **1/9** the additional reflections completely disappear at the next phase transition at $T = 50$ °C (Fig. 12d). This phase transition ($\Delta H =$ 0.6 kJ mol^{-1}) is associated with a significant increase of the intensity of the small angle scattering, which can now be regarded as a sharp layer reflection with $d = 3.52$ nm. In addition, a further increase of the tilt angle from 28° in the CybC phase to 31–32° and the occurrence of second order layer reflections is observed (see Fig. 12d). This indicates the transition to a proper smectic phase ($SmC_{(I)}$) *i.e.* this transition is assigned to the complete fusion of the cybotactic clusters to quasi-infinite layers.

Though several phase transitions can be observed in the mesomorphic range between 50 and 104 °C, no significant change of the shape and intensity of the diffuse wide angle scattering can be detected. There is only an apparently continuous shift of the maximum of the diffuse wide angle scattering from 0.46 nm at 110 °C to 0.45 nm at 45 °C (Fig. 5c and S9b†),

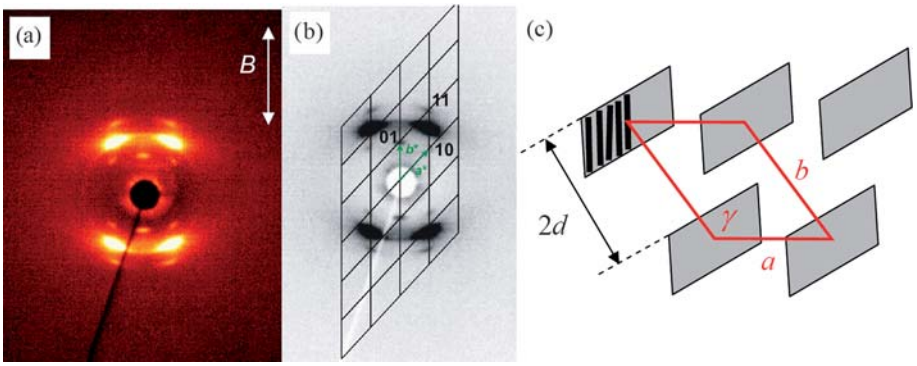

Fig. 13 X-Ray diffraction patterns of a sample of the CybC phase of compound **2** aligned in the magnetic field: (a) small angle diffraction pattern at $T =$ 45 °C; (b) same pattern with reciprocal lattice and indexation; (c) model of the organization of the molecules (grey ribbons identify the positions of the aromatic cores, a, b and γ indicate the 2D lattice, d is the d-value measured for the more diffuse small angle scatterings of the less ordered regions (added for comparison and does not belong to the 2D lattice); the space in the defects between the ribbons in horizontal direction might be filled by additional only orientationally ordered molecules).

indicating that all mesophases represent fluid LC phases and that there is only a slight increase of the packing density in the whole temperature range.

A similar phase sequence as found for **1/9** and **2** was observed for compounds **1/8** (see Fig. S7†) and **1/7** (but in this case no 2D lattice could be observed by XRD, Fig. S6d†). Hence, the CybC phase can be regarded as an intermediate phase at the transition from cybotactic nematic to proper smectic phases of bent-core molecules.

3.3.2 Compounds 1/10–1/14 with long chains. For compound **1/10** and the higher homologues a similar phase sequence was observed (for textural changes see Fig. S20†), where at a first transition the small angle X-ray scattering remains relatively diffuse and in a second step a SmC phase with sharp layer reflections is formed (see Fig. 14 and 15). However, there are also differences to the behaviour of compounds **1/7–1/9** and **2** with shorter chains. For compound **1/10** the tilt angle increases only slightly at the N_{cyb}-to-CybC transition from about 15–16° to 18–20°; this is a much smaller increase compared to **1/9**. In addition, the intensity of the small angle diffractions at the left and the right becomes different at this transition (Fig. 14b) indicating the occurrence of a nonequal distribution of the tilt directions, whereas for the medium chain compounds **1/7–1/9** and **2** the intensity distribution of the small angle scattering did not change. Moreover, for compound **1/10** and for all higher homologues the additional spot-like small angle scattering is completely missing. It can be assumed that the phase structure is similar to the CybC phases of compounds **1/8**, **1/9** and **2**, but in this case no 2D lattice can be observed under the applied experimental conditions. This might be due to a stronger influence of surface anchoring provided by the larger clusters, which in the CybC phases of these compounds could lead to a predominance of a distinct tilt direction and to distortion of the alignment by the magnetic field.

At the next phase transition at $T = 67$ °C the layer reflection becomes significantly sharper and weak second order layer reflections can be found (Fig. 14c), indicating the transition to a true SmC phase composed of quasi-infinite layers ($SmC_{(I)}$), very similar to the CybC-to-$SmC_{(I)}$ transition observed for **1/9**. This transition is associated with only a slight increase of the tilt angle from 20 to 24–25° (Fig. 15a). The reduced X-ray tilt in the smectic phases of the long chain compounds could be due to the growing importance of the alkyl chains which are more disordered and decrease the tilt observable by XRD (see discussion in Section 3.2.1). Moreover, the position of the diffuse wide angle scattering changes with respect to the equator (yellow dotted lines in Fig. 14) indicating a change of the alignment of the molecules. This might also be a result of the increased impact of surface alignment upon layer orientation, leading to a deviation from the alignment induced by the magnetic field.[75]

The additional transition at $T = 58$ °C is associated with an increase of the intensity of the second order layer reflection and a further increase of the tilt of the layers with respect to the magnetic field direction (Fig. 14d), though the tilt angle of the molecules in the layers remains nearly constant between 24 and 25° (Fig. 15a). Again, in the whole temperature range there is no significant change in the diffuse wide angle scattering, it remains completely diffuse so that all mesophases represent fluid LC phases. The maximum of the wide angle scattering is shifted in the temperature range between 100 °C and 50 °C only from 0.46 nm at 100 °C to 0.45 nm at 50 °C (Fig. 15c).

With further increasing chain length the changes occurring at the phase transitions become more and more difficult to recognize. However, by comparing the diffraction patterns, textures and the development of the tilt angles (see Fig. S11–S16 and Tables S8–S10†), the phase assignment shown in Table 1 was deduced. Accordingly, the phase behaviour of compounds **1/10–1/14** is similar to each other and characterized by a phase sequence Iso–N_{cybC}–CybC–$SmC_{(I)}$–$SmC_{(II)}$ on cooling, whereby all phase transition temperatures and also the associated enthalpy values increase with growing chain length. In some cases the $SmC_{(II)}$ phase cannot be observed, due to crystallization of the sample and for compound **1/14** there seems to be an additional low temperature phase M which could not be investigated in detail due to partial crystallization.

Electro-optical investigations indicate that no polar switching is observed in the whole mesomorphic temperature range (voltages up to 400 V_{pp} in 6 μm cells) of all compounds **1/*n***. Hence, in

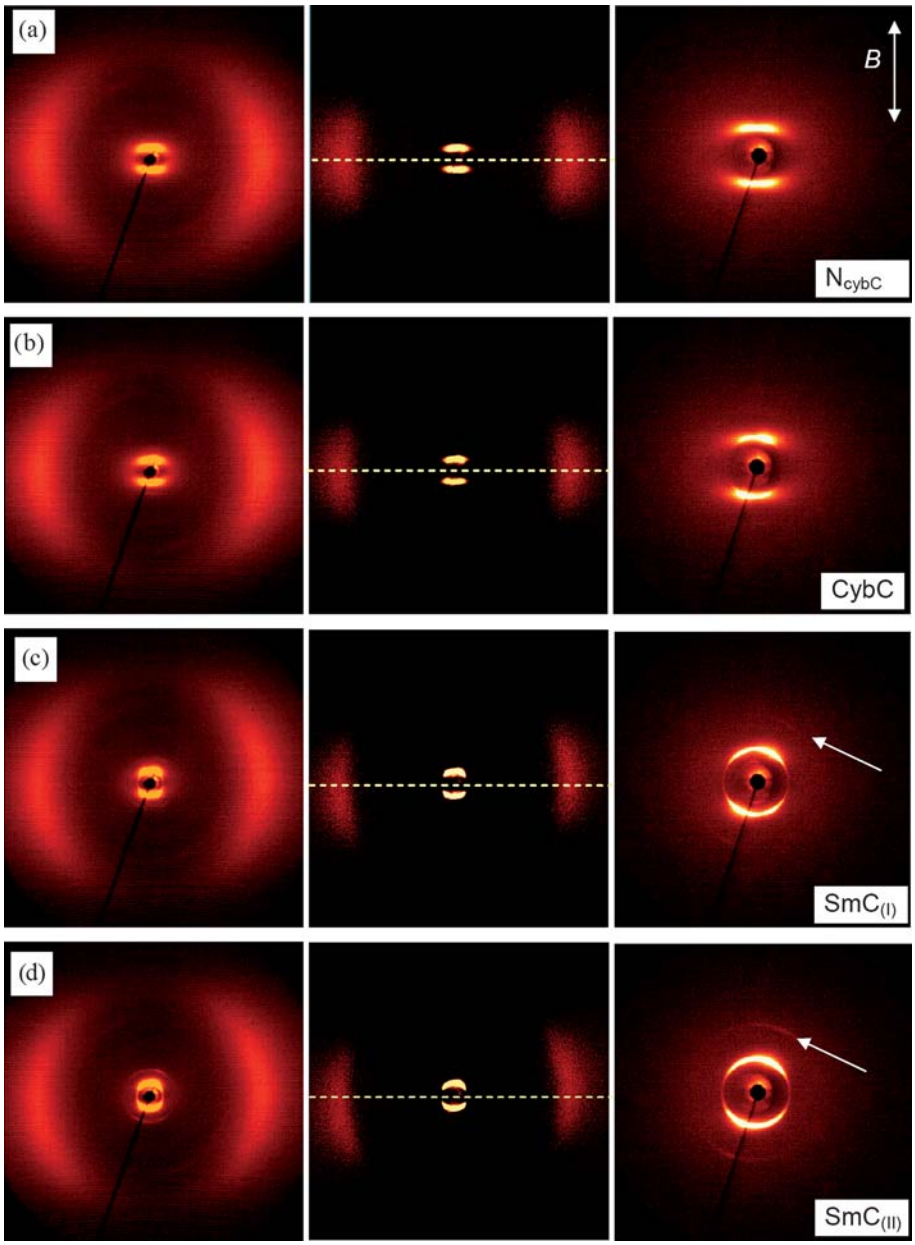

Fig. 14 X-Ray diffraction patterns (wide angle pattern at the left, wide angle scattering after subtraction of the isotropic in the middle and small angle pattern at the right) of a sample of compound **1/10** aligned in the magnetic field: (a) N_{cybC} phase at 95 °C; (b) CybC phase at 80 °C; (c) $SmC_{(I)}$ phase at 60 °C and (d) $SmC_{(II)}$ phase at 53 °C; in (c) and (d) the arrows indicate the position of the second order layer reflection.

these LC phases the aromatic cores do not adopt long-range polar order. This behaviour is distinct from the analogous alkoxy substituted compounds where on decreasing temperature the nematic phase is first replaced by a nonpolar SmC phase, followed by an antiferroelectric switching polar $SmCP_A$ phase.[48] This observation could be explained by a different packing density of the aromatics due to the lower rotational barrier of the Ar–CH_2 bond compared to the Ar–O bond,[76] the distinct conformations[77] and the increased polarizability of the alkyoxy substituted aromatic cores.[78] These effects lead to a less dense packing of the alkyl substituted compounds **1/*n*** compared to the more densely packed alkoxy substituted compounds, resulting in modifications of the phase structures and loss of polar order.

4. Summary and conclusions

New bent-core mesogens with broad nematic phase ranges (enantiotropic and monotropic), some of them long-term metastable at ambient temperature and without smectic low temperature phases, have been obtained in a homologous series of alkyl substituted 4-cyanoresorcinol bisbenzoates **1/*n***. Mixtures of these compounds could possibly lead to bent-core materials with stable nematic phases around room temperature. Moreover, compounds **1/2** and **1/3** belong to the bent-core mesogens with the shortest terminal chains reported so far.[79] The systematic investigation of the structure of the nematic phases depending on chain length revealed a chain length dependent structural

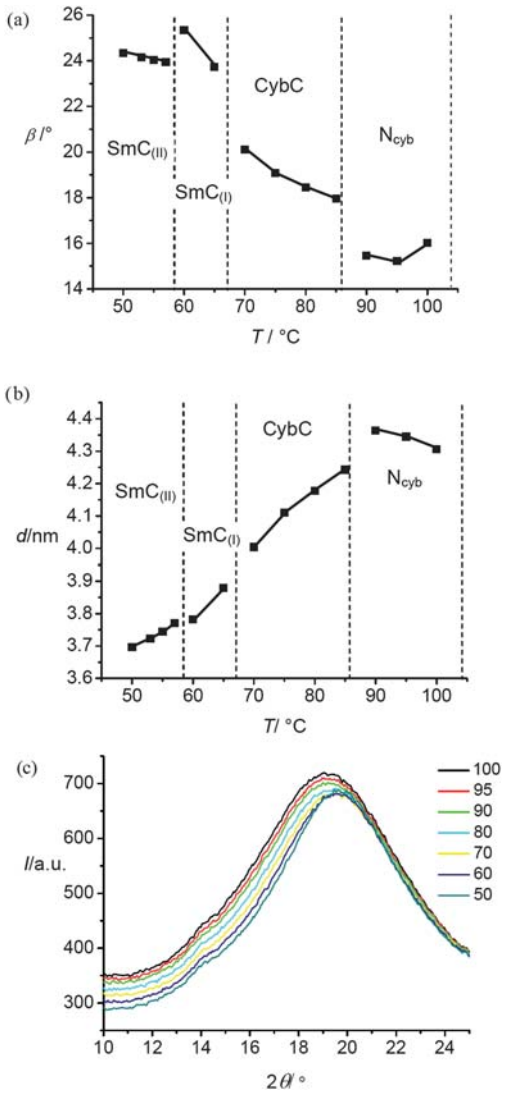

Fig. 15 X-Ray data of compound **1/10**: (a) development of the tilt angle β (in the smectic phases determined from the positions of the small angle maxima with respect to the wide angle maxima, in the N_{cybC} phase deduced from the splitting of the small angle scattering $\Delta\chi/2$); (b) temperature dependence of *d*-values of the maxima of the small angle scattering; (c) θ-scans over the diffuse wide angle scattering (100, 95 °C: N_{cybC}; 90, 80, 70 °C: CybC; 60 °C: $SmC_{(I)}$; 50 °C: $SmC_{(II)}$; the small shoulder at $2\theta = 14°$ is an artefact due to the magnetic oven).

transformation from nematic phases with only nearest neighbour correlations, similar to ordinary nematic phases (**1/2–1/4**), to cybotactic nematic phases composed of large clusters (**1/10–1/14**). Medium chain compounds (**1/6–1/9**) have a strong temperature dependence of cluster size, indicating a temperature dependent structural transformation. Cluster formation is mainly caused by the segregation of the alkyl chains and supported by the kink-shape of the molecules. The change of the cluster size leads to distinct changes of the properties of the nematic phases (alignment behaviour, viscosity, *etc.*) and this provides explanations for some temperature dependent phenomena (*e.g.* textural changes) which should not be misinterpreted as indications of N_u–N_b transitions. Though for none of the nematic phases spontaneous biaxiality could be confirmed, there are recent indications of induced biaxiality.[69] The deeper understanding of the molecular organization in the nematic phases of bent-core molecules also provides a basis for future materials design of biaxial nematic materials. The proven cluster structure is favourable for development of N_b phases for long and medium chain compounds, but the tilted organization in the N_{cybC} phases could only lead to N_b phases with C_{2h} symmetry (N_{bm} phases, see Fig. 1c). These N_{bm} phases are difficult to distinguish from improper phase biaxiality which is exclusively based on the tilted organization of the molecules in SmC type clusters. Proof of proper biaxiality (significantly restricted rotation around **n**) would in this case require ^{2}H NMR studies with selectively deuterated samples. However, for practical applications nontilted N_b phases with D_{2h} symmetry would be much more useful. These could probably be achieved with N phases of short chain compounds, but phase biaxiality is less likely to appear in molecular nematic phases.[15] Therefore, the design of nontilted cybotactic nematic phases (N_{cybA}) is a desirable target.

Overall, this work has contributed to the clarification of the confusion concerning the interpretation of the four spot patterns often observed in the small angle XRD patterns of nematic phases of bent-core mesogens. Accordingly, in the ordinary nematic phases with only nearest neighbour correlation, formed by compounds with very short terminal chains, it seems to originate from the distinct orientation of the rod-like wings of the bent cores,[80] whereas it is due to the tilt of the director **n** in the SmC type clusters in the N_{cybC} phases of molecules with long alkyl chains. For bent-core molecules with a medium chain length the tilt as well as the bending angle contribute to the small angle splitting and there is a strong temperature dependence of cluster size and observed splitting. Hence, for the short and medium chain bent-core compounds the measured angular splitting seems to be not directly related to the tilt angle of the molecules in the cybotactic clusters. In any case, this four spot pattern cannot be considered as an indication of phase biaxiality.

It was also found that the transition from the cybotactic nematic to smectic phases, occurring on further chain elongation and temperature reduction, takes place in a sequence of two subsequent steps. At first an intermediate phase composed of elongated cybotactic clusters (CybC) is formed, followed by a fusion of these ribbon-like aggregates to quasi-infinite layers in the proper smectic C phases ($SmC_{(I)}$), which on further cooling can adopt a slightly denser packing of the molecules ($SmC_{(II)}$). However, none of these phases shows polar order, which requires a further increase of the packing density.

Hence, materials design by systematic variation of bent-core based mesogenic tectons lead to an improved understanding of the nature of the nematic phases of bent-core mesogens and to the discovery of new modes of self-assembly at the nematic–smectic cross-over. This might have an impact on the general understanding of phase transitions in soft matter systems as well as it contributes more specifically to the development of basic designing principles to achieve spontaneous or field induced biaxial nematic bent-core based materials with low transition temperatures.

Acknowledgements

This work was supported by the EU within the FP7 funded Collaborative Project BIND (grant no. 216025); C. K. is grateful

to Alexander von Humboldt-foundation for a Feodor Lynen-fellowship.

References

1 M. J. Freiser, *Phys. Rev. Lett.*, 1970, **24**, 1041.
2 Reviews: G. R. Luckhurst, *Thin Solid Films*, 2001, **393**, 40; K. Praefcke, *Mol. Cryst. Liq. Cryst.*, 2001, **364**, 15; G. R. Luckhurst, *Angew. Chem., Int. Ed.*, 2005, **44**, 2834; D. W. Bruce, *Chem. Rec.*, 2004, **4**, 10.
3 Y. Galerne, *Mol. Cryst. Liq. Cryst.*, 1998, **323**, 211.
4 R. Berardi, L. Muccioli and C. Zannoni, *J. Chem. Phys.*, 2008, **128**, 024905.
5 R. Berardi and C. Zannoni, *J. Chem. Phys.*, 2000, **113**, 5971; R. Berardi, L. Muccioli, S. Orlandi, M. Ricci and C. Zannoni, *J. Phys.: Condens. Matter*, 2008, **20**, 463101.
6 T. C. Lubensky and L. Radzihovsky, *Phys. Rev. E: Stat., Nonlinear, Soft Matter Phys.*, 2002, **66**, 031704.
7 (*a*) R. Alben, *Phys. Rev. Lett.*, 1973, **30**, 778; (*b*) R. Alben, *J. Chem. Phys.*, 1973, **59**, 4299; (*c*) J. P. Straley, *Phys. Rev. A: At., Mol., Opt. Phys.*, 1974, **10**, 1881; M. P. Taylor and J. Herzfeld, *Phys. Rev. A: At., Mol., Opt. Phys.*, 1991, **44**, 3742; H. H. Wensink, G. J. Vroege and H. N. W. Lekkerkerker, *Phys. Rev. E: Stat., Nonlinear, Soft Matter Phys.*, 2002, **66**, 041704.
8 I. D. Fletcher and G. R. Luckhurst, *Liq. Cryst.*, 1995, **18**, 175; J. Hunt, R. W. Date, B. A. Timini, G. R. Luckhurst and D. W. Bruce, *J. Am. Chem. Soc.*, 2001, **123**, 10115; R. W. Date and D. W. Bruce, *J. Am. Chem. Soc.*, 2003, **125**, 9012; P. H. J. Kouwer and G. H. Mehl, *J. Mater. Chem.*, 2009, **19**, 1564; P. H. J. Kouwer and G. H. Mehl, *J. Am. Chem. Soc.*, 2003, **125**, 11172; D. Apreutesei and G. H. Mehl, *Chem. Commun.*, 2006, 609.
9 K.-U. Jeong, A. J. Jing, B. Mansdorf, M. J. Graham, D.-K. Yang, F. W. Harris and S. Z. D. Cheng, *Chem. Mater.*, 2007, **19**, 2921.
10 S. Chandrasekhar, G. Nair, D. S. S. Rao, S. K. Prasad, K. Praefcke and D. Singer, *Mol. Cryst. Liq. Cryst.*, 1996, **288**, 7; J. Malthete, L. Liebert, A. M. Levelut and Y. Galerne, *C. R. Acad. Sci., Ser. II: Mec., Phys., Chim., Sci. Terre Univers.*, 1986, **303**, 1073; K. Praefcke, B. Kohne, D. Singer, D. Demus, G. Pelzl and S. Diele, *Liq. Cryst.*, 1990, **7**, 589.
11 K. Merkel, A. Kocot, J. K. Vij, R. Korlacki, G. H. Mehl and T. Meyer, *Phys. Rev. Lett.*, 2004, **93**, 237801; J. L. Figueirinhas, C. Cruz, D. Filip, G. Feio, A. C. Ribeiro, Y. Frere, T. Meyer and G. H. Mehl, *Phys. Rev. Lett.*, 2005, **94**, 107802; K. Neupane, S. W. Kang, S. Sharma, D. Carney, T. Meyer, G. H. Mehl, D. W. Allender, S. Kumar and S. Sprunt, *Phys. Rev. Lett.*, 2006, **97**, 207802; C. Cruz, J. L. Figueirinhas, D. Filip, G. Feio, A. C. Ribeiro, Y. Frere, T. Meyer and G. H. Mehl, *Phys. Rev. E: Stat., Nonlinear, Soft Matter Phys.*, 2008, **78**, 051702; M. Cardoso, J. L. Figueirinhas, C. Cruz, A. Van-Quynh, A. C. Ribeiro, G. Feio, D. Apreutesei and G. H. Mehl, *Mol. Cryst. Liq. Cryst.*, 2008, **495**, 348; G. Cordoyiannis, D. Apreutesei, G. H. Mehl, C. Glorieux and J. Thoen, *Phys. Rev. E: Stat., Nonlinear, Soft Matter Phys.*, 2008, **78**, 011708.
12 F. Hessel and H. Finkelmann, *Polym. Bull.*, 1986, **15**, 349; H. F. Leube and H. Finkelmann, *Makromol. Chem.*, 1991, **192**, 1317; K. Severing and K. Saalwächter, *Phys. Rev. Lett.*, 2004, **92**, 125501; K. Severing, E. Stibal-Fischer, A. Hasenhindl, H. Finkelmann and K. Saalwächter, *J. Phys. Chem.*, 2006, **110**, 15680; R. Storz, A. Komp, A. Hoffmann and H. Finkelmann, *Macromol. Rapid Commun.*, 2009, **30**, 615.
13 (*a*) L. A. Madsen, T. J. Dingemans, M. Nakata and E. T. Samulski, *Phys. Rev. Lett.*, 2004, **92**, 145505; (*b*) B. R. Acharya, A. Primak and S. Kumar, *Phys. Rev. Lett.*, 2004, **92**, 145506; (*c*) B. R. Acharya, A. Primak, T. J. Dingemans, E. T. Samulski and S. Kumar, *Pramana*, 2003, **61**, 231; (*d*) L. A. Madsen, T. J. Dingemans, M. Nakata and E. T. Samulski, *Phys. Rev. Lett.*, 2006, **96**, 219804; (*e*) Y. Galerne, *Phys. Rev. Lett.*, 2006, **96**, 219803.
14 B. Mettout, *Phys. Rev. E: Stat., Nonlinear, Soft Matter Phys.*, 2005, **72**, 031706; M. A. Bates and G. R. Luckhurst, *Phys. Rev. E: Stat., Nonlinear, Soft Matter Phys.*, 2005, **72**, 051702; M. A. Bates, *Chem. Phys. Lett.*, 2007, **437**, 189.
15 A. G. Vanakaras and D. J. Photinos, *J. Chem. Phys.*, 2008, **128**, 154512; S. D. Peroukidis, P. K. Karahaliou, A. G. Vanakaras and D. J. Photinos, *Liq. Cryst.*, 2009, **36**, 727; P. K. Karahaliou, A. G. Vanakaras and D. J. Photinos, *J. Chem. Phys.*, 2009, **131**, 124516.
16 P. K. Karahaliou, P. H. J. Kouwer, T. Meyer, G. H. Mehl and D. J. Photinos, *J. Phys. Chem.*, 2008, **112**, 6550.
17 R. Barberi, F. Ciuchi, G. Lombardo, R. Bartolino and G. E. Durand, *Phys. Rev. Lett.*, 2004, **93**, 137801.
18 J.-H. Lee, T.-K. Lim, W.-T. Kim and J.-I. Jin, *J. Appl. Phys.*, 2007, **101**, 034105; R. Stanarius, *J. Appl. Phys.*, 2008, **104**, 036104; J. You, J. Y. Jung, K. Rhie, V. M. Pergamenschik and S. T. Shin, *J. Korean Phys. Soc.*, 2008, **52**, 342; G. S. Lee, J. S. Cho, J. C. Kim, T.-H. Yoon and S. T. Shin, *J. Appl. Phys.*, 2009, **105**, 094509.
19 J. A. Olivares, S. Stojadinovic, T. Dingemans, S. Sprunt and A. Jakli, *Phys. Rev. E: Stat., Nonlinear, Soft Matter Phys.*, 2003, **68**, 041704.
20 Field induced polar order and hence biaxiality were observed in optical uniaxial smectic phases composed of polar clusterseither (a) with tilted arrangement of the molecules in these clusters ($SmCP_R$, see: G. Dantlgraber, U. Baumeister, S. Diele, H. Kresse, B. Lühmann, H. Lang and C. Tschierske, *J. Am. Chem. Soc.*, 2002, **124**, 14852) or (b) with nontilted organization of the molecules ($SmAP_R$, see: Y. Shimbo, E. Gorecka, D. Pociecha, F. Araoka, M. Goto, Y. Takanishi, K. Ishikawa, J. Mieczkowski, K. Gomola and H. Takezoe, *Phys. Rev. Lett.*, 2006, **97**, 113901).
21 R. Stannarius, A. Eremin, M.-G. Tamba, G. Pelzl and W. Weissflog, *Phys. Rev. E: Stat., Nonlinear, Soft Matter Phys.*, 2007, **76**, 061704.
22 Reviews: (*a*) R. Amaranatha Reddy and C. Tschierske, *J. Mater. Chem.*, 2006, **16**, 907; (*b*) H. Takezoe and Y. Takanishi, *Jpn. J. Appl. Phys.*, 2006, **45**, 597; (*c*) J. Etxebarria and M. Blanca, *J. Mater. Chem.*, 2008, **18**, 2919.
23 M. Lehmann and J. Levin, *Mol. Cryst. Liq. Cryst.*, 2004, **411**, 273; M. Lehmann, S.-W. Kang, C. Köhn, S. Haseloh, U. Kolb, D. Schollmeyer, Q. Wang and S. Kumar, *J. Mater. Chem.*, 2006, **16**, 4326; M. Lehmann, C. Köhn, H. Kresse and Z. Vakhovskaya, *Chem. Commun.*, 2008, 1768; M. Lehmann, J. Seltmann, A. A. Auer, E. Prochnow and U. Benedikt, *J. Mater. Chem.*, 2009, **19**, 1978.
24 V. Prasad, S.-W. Kang, K. A. Suresh, L. Joshi, Q. Wang and S. Kumar, *J. Am. Chem. Soc.*, 2005, **127**, 17224.
25 T. J. Dingemanns, L. A. Madsen, N. A. Zafiropoulos, W. Lin and E. T. Samulski, *Philos. Trans. R. Soc. London, Ser. A*, 2006, **364**, 2681; N. A. Zafiropoulos, W. Lin, E. T. Samulskii, T. J. Dingemans and S. J. Picken, *Liq. Cryst.*, 2009, **36**, 649.
26 (*a*) B. R. Acharya, S.-W. Kang and S. Kumar, *Liq. Cryst.*, 2008, **35**, 109; (*b*) B. R. Acharya, A. S.-W. Kang, V. Prasad and S. Kumar, *J. Phys. Chem. B*, 2009, **113**, 3845.
27 C. V. Yelamaggad, S. Shashikala, D. S. Shankar Rao, C. V. Lobo and S. Chandrasekhar, *Angew. Chem., Int. Ed.*, 2004, **43**, 3429; M. G. Tamba, B. Kosata, K. Pelz, S. Diele, G. Pelzl, Z. Vakhovskaya, H. Kresse and W. Weissflog, *Soft Matter*, 2006, **2**, 60.
28 C. D. Southern, P. D. Brimicombe, S. D. Siemianowski, S. Jaradat, N. Roberts, V. Görtz, J. W. Goodby and H. F. Gleeson, *Europhys. Lett.*, 2008, **82**, 56001; Y. Xiang, J. W. Goodby, V. Görtz and H. F. Gleeson, *Appl. Phys. Lett.*, 2009, **94**, 193507.
29 (*a*) S. I. Torgova, T. A. Geivandova, O. Francescangeli and A. Strigazzi, *Pramana*, 2003, **61**, 239; (*b*) O. Francescangeli, V. Stanic, S. I. Torgova, A. Strigazzi, N. Scaramuzza, C. Ferrero, I. P. Dolbnya, T. M. Weiss, R. Berardi, L. Muccioli, S. Orlandi and C. Zannoni, *Adv. Funct. Mater.*, 2009, **19**, 2592.
30 Amplification of chirality as expressed by induction of blue phases by achiral bent-core mesogens in a cholesteric host system: J. Thisayukta, H. Niwano, H. Takezoe and J. Watanabe, *J. Am. Chem. Soc.*, 2002, **124**, 3354; M. Nakata, Y. Takanishi, J. Watanabe and H. Takezoe, *Phys. Rev. E: Stat., Nonlinear, Soft Matter Phys.*, 2003, **68**, 041710.
31 Surface induced or intrinsic chirality in nematic phases of achiral bent core mesogens: (*a*) G. Pelzl, A. Eremin, S. Diele, H. Kresse and W. Weissflog, *J. Mater. Chem.*, 2002, **12**, 2591; (*b*) T. Niori, J. Yamamoto and H. Yokoyama, *Mol. Cryst. Liq. Cryst.*, 2004, **409**, 475; (*c*) V. Görtz and J. W. Goodby, *Chem. Commun.*, 2005, 3262; (*d*) C. Praasang, A. C. Whitwood and D. W. Bruce, *Chem. Commun.*, 2008, 2137; (*e*) P. S. Salter, P. W. Benzie, R. A. Reddy, C. Tschierske, S. J. Elston and E. P. Raynes, *Phys. Rev. E: Stat., Nonlinear, Soft Matter Phys.*, 2009, **80**, 031701.
32 J. Harden, B. Mbanga, N. Eber, K. Fodor-Csorba, S. Sprunt, J. T. Gleeson and A. Jakli, *Phys. Rev. Lett.*, 2006, **97**, 157802.

33 P. Kumar, Y. G. Marinov, H. P. Hinov, U. S. Hiremath, C. V. Yelamaggad, K. S. Krishnamurthy and A. G. Petrov, *J. Phys. Chem. B*, 2009, **113**, 9168.

34 (*a*) D. Wiant, J. T. Gleeson, N. Éber, K. Fodor-Csorba, A. Jákli and T. Tóth-Katona, *Phys. Rev. E: Stat., Nonlinear, Soft Matter Phys.*, 2005, **72**, 041712; (*b*) P. Kumar, U. S. Hiremath, C. V. Yelamaggad, A. G. Rossberg and K. S. Krishnamurthy, *J. Phys. Chem. B*, 2008, **112**, 9753; (*c*) P. Kumar, U. S. Hiremath, C. V. Yelamaggad, A. G. Rossberg and K. S. Krishnamurthy, *J. Phys. Chem. B*, 2008, **112**, 9270; (*d*) J. Heuer, R. Stannarius, M.-G. Tamba and W. Weissflog, *Phys. Rev. E: Stat., Nonlinear, Soft Matter Phys.*, 2008, **77**, 056206; (*e*) S. Tanaka, S. Dhara, B. K. Sadashiva, Y. Shimbo, Y. Takanishi, F. Araoka, K. Ishikawa and H. Takezoe, *Phys. Rev. E: Stat., Nonlinear, Soft Matter Phys.*, 2008, **77**, 041708.

35 (*a*) E. Dorjgotov, K. Fodor-Csorba, J. T. Gleeson, S. Sprunt and A. Jakli, *Liq. Cryst.*, 2008, **35**, 149; (*b*) C. Bailey, K. Fodor-Csorba, J. T. Gleeson, S. Sprunt and A. Jakli, *Soft Matter*, 2009, **5**, 3618.

36 (*a*) A. de Vries, *Pramana*, 1975, **1**, 93; (*b*) A. de Vries, *J. Mol. Liq.*, 1986, **31**, 193; (*c*) P. Sarkar, P. K. Sarkar, S. Paul and P. Mandal, *Phase Transitions*, 2000, **71**, 1.

37 O. Francescangeli, M. Laus and G. Galli, *Phys. Rev. E: Stat. Phys., Plasmas, Fluids, Relat. Interdiscip. Top.*, 1997, **55**, 481487.

38 S. Stojadinovic, A. Adorjan, S. Sprunt, H. Sawade and A. Jakli, *Phys. Rev. E: Stat., Nonlinear, Soft Matter Phys.*, 2002, **66**, 060701; D. Wiant, S. Stojadinovic, K. Neupane, S. Sharma, K. Fodor-Csorba, A. Jakli, J. T. Gleeson and S. Sprunt, *Phys. Rev. E: Stat., Nonlinear, Soft Matter Phys.*, 2006, **73**, 030703.

39 There is also no clear difference between "classical" nematic phases and those based on cybotactic clusters as in all cases there is at least some (nearest neighbour) aggregations of the molecules and the transition between these two substructures of nematic phases is continuous. However, considering the possibility of surface and field induced phase biaxiality in nematic phases it is important to know the size of the clusters as in nematic phases with strong clustering, field- and surface-induced biaxial order becomes much more likely due to the cooperativity provided in clusters[29b].

40 Cybotactic nematic phases can in fact also be found quite often for rod-like mesogens, not only as a pretransitional phenomenon at the transition to smectic phases, but also over broad temperature ranges. This type of nematic phases was reported for various types of mesogenic materials, as for example for rod-like molecules with extended rigid cores and with relatively strong attraction between the rigid cores *e.g.* mesognenic dimers of benzoic acids (V. A. Gudkov, *J. Struct. Chem.*, 1992, **33**, 436), nitrophenyl benzoates (T. Tasaka, V. F. Petrov, H. Okamoto, Y. Morita, K. Suetake and S. Takenaka, *Liq. Cryst.*, 2002, **29**, 1311), cyanobiphenyls (A. J. Leadbetter, R. M. Richardson and C. N. Colling, *J. Phys. Colloq.*, 1975, **36**, 37), as well as for calamitic mesogens with preorganized aromatic cores, as for example in LC polymers, dendrimers (V. Percec, P. Chu, G. Ungar and J. Zhou, *J. Am. Chem. Soc.*, 1995, **117**, 11441) and for oligomesogens (S. K. Pal, V. A. Raghunathan and S. Kumar, *Liq. Cryst.*, 2007, **34**, 135; ref. 16). Also for the nematic phases of bent-core mesogens it seems to be the predominating mode of organization due to the high aggregation tendency of their aromatic cores.

41 D. Shen, S. Diele, G. Pelzl, I. Wirth and C. Tschierske, *J. Mater. Chem.*, 1999, **9**, 661.

42 (*a*) R. Amaranatha Reddy and B. K. Sadashiva, *Liq. Cryst.*, 2000, **27**, 1613; (*b*) R. Amaranatha Reddy, B. K. Sadashiva and V. A. Raghunathan, *Chem. Mater.*, 2004, **16**, 4050; (*c*) S. Murthy and B. K. Sadashiva, *Liq. Cryst.*, 2004, **31**, 1347; (*d*) R. Amaranatha Reddy and B. K. Sadashiva, *J. Mater. Chem.*, 2004, **14**, 1936; M. Kohout, J. Svoboda, V. Novotna, D. Pociecha, M. Glogarova and E. Gorecka, *J. Mater. Chem.*, 2009, **19**, 3153; N. S. Novikova, E. Gorecka, R. V. Kondratyeva and E. D. Kilimenchuk, *Liq. Cryst.*, 2008, **35**, 743; S. K. Lee, X. Li, S. Kang, M. Tokita and J. Watanabe, *J. Mater. Chem.*, 2009, **19**, 4517.

43 D. Apreutesei and G. H. Mehl, *J. Mater. Chem.*, 2007, **17**, 4711.

44 S. Kang, Y. Saito, N. Watanabe, M. Tokita, Y. Takanishi, H. Takezoe and J. Watanabe, *J. Phys. Chem. B*, 2006, **110**, 5205.

45 (*a*) M. W. Schröder, S. Diele, G. Pelzl, U. Dunemann, H. Kresse and W. Weissflog, *J. Mater. Chem.*, 2003, **13**, 1877; (*b*) F. C. Yu and L. J. Yu, *Liq. Cryst.*, 2008, **35**, 799; (*c*) F. C. Yu and L. J. Yu, *Chem. Mater.*, 2006, **18**, 5410; (*d*) V. Novotna, J. Zurek, V. Kozmık, J. Svoboda, M. Glogarova, J. Kroupa and D. Pociecha, *Liq. Cryst.*, 2008, **35**, 1023.

46 C. V. Yelamaggad, I. S. Shashikala, G. Liao, D. S. Shankar Rao, S. Krishna Prasad, Q. Li and A. Jakli, *Chem. Mater.*, 2006, **18**, 6100.

47 I. Wirth, S. Diele, A. Eremin, G. Pelzl, S. Grande, L. Kovalenko, N. Pancenko and W. Weissflog, *J. Mater. Chem.*, 2001, **11**, 1642.

48 L. Kovalenko, M. W. Schröder, R. A. Reddy, S. Diele, G. Pelzl and W. Weissflog, *Liq. Cryst.*, 2005, **32**, 857.

49 W. Weissflog, N. Nadasi, U. Dunemann, G. Pelzl, S. Diele, A. Eremin and H. Kresse, *J. Mater. Chem.*, 2001, **11**, 2748; U. Dunemann, M. W. Schröder, R. Amaranatha Reddy, G. Pelzl, S. Diele and W. Weissflog, *J. Mater. Chem.*, 2005, **15**, 4051; W. Weissflog, H. N. Shreenivasa Murthy, S. Diele and G. Pelzl, *Philos. Trans. R. Soc. London, Ser. A*, 2006, **364**, 2657; G. Pelzl and W. Weissflog, in *Thermotropic Liquid Crystals, Recent Advances*, ed. A. Ramamoorthy, Springer, Dordrecht, Netherlands, 2007, pp.1–58.

50 W. Weissflog, S. Sokolowski, H. Dehne, B. Das, S. Grande, M. W. Schröder, A. Eremin, S. Diele, G. Pelzl and H. Kresse, *Liq. Cryst.*, 2004, **31**, 923.

51 B. Kosata, G.-M. Tamba, U. Baumeister, K. Pelz, S. Diele, G. Pelzl, G. Galli, S. Samaritani, E. V. Agina, N. I. Boiko, V. P. Shibaev and W. Weissflog, *Chem. Mater.*, 2006, **18**, 691.

52 D. Shen, A. Pegenau, S. Diele, I. Wirth and C. Tschierske, *J. Am. Chem. Soc.*, 2000, **122**, 1593; R. Achten, R. Cuypers, M. Giesbers, A. Koudijs, A. T. M. Marcelis and E. J. R. Sudhölter, *Liq. Cryst.*, 2004, **31**, 1167.

53 (*a*) B. Neises and W. Steglich, *Angew. Chem., Int. Ed. Engl.*, 1978, **17**, 522; (*b*) J. C. Sheehan and J. J. Hlavka, *J. Org. Chem.*, 1956, **21**, 439; (*c*) C. Tschierske and H. Zaschke, *J. Prakt. Chem.*, 1989, **331**, 365.

54 (*a*) E. Marcus, *Chem. Ber.*, 1891, **24**, 3650; (*b*) J. L. Serrano, T. Sierra, Y. Gonzalez, C. Bolm, K. Weickardt, A. Magnus and G. Moll, *J. Am. Chem. Soc.*, 1995, **117**, 8312.

55 R. Achten, A. Koudijs, M. Giesbers, A. T. Marcelis and E. J. R. Sudhölter, *Liq. Cryst.*, 2005, **32**, 277; G. S. Lee, Y.-J. Lee, S. Y. Choi, Y. S. Park and K. B. Yoon, *J. Am. Chem. Soc.*, 2000, **122**, 12151.

56 Remarkably, this odd–even effect is reversed to that observed for linear rod-like molecules, where higher mesophase stabilities were found for molecules with even numbered chains. This might be due to the fact that for these bent molecules a slightly bent conformation of the terminal chains can reduce the overall bending angle and in this way stabilizes the mesophase by an increase of the molecular length to broadness ratio.

57 As determined by NMR investigations for related 4-cyanoresorcinol bisbenzoates with Schiff base wings[47].

58 J. D. Litster, *Philos. Trans. R. Soc. London, Ser. A*, 1983, **309**, 145–153.

59 A. Guinier, *X-Ray Diffraction*, Freeman, San Francisco, 1963.

60 Abbreviations: K is the Scherrer constant; λ is the wavelength of the incident radiation; θ_B is the Bragg angle; and $\Delta(2\theta)_{\|}$ and $\Delta(2\theta)\perp$ are the FWHMs of the diffraction peak measured in the longitudinal and transversal direction[37].

61 These relatively narrow line shapes of the N_{cybC} phases of long chain compounds would require experiments with a synchrotron source and deconvolution of the instrumental line shape before calculating the correlation length.

62 The lateral distance is more uncertain as the scattering in this direction is strongly influenced by the quality of alignment, hence this number might actually be a bit smaller; it must also be considered that the magnetic field has a significant influence on alignment and correlation length;[29b] as the correlation lengths increase with increasing field strength, a uniform field strength of $B \approx 1$ T was used in all XRD investigations to achieve comparability.

63 These values are in good agreement with those obtained in synchrotron experiments with cybotactic nematic phases of oxadiazole based bent core mesogens with a similar chain length, where correlation lengths $\xi_{\|} = 3.0$ to 4.7 nm ($L_{\|} = 9$–14 nm) and $\xi\perp = 1.5$ to 2.5 nm ($L_{\perp} = 4.5$–7.5 nm) were determined in samples aligned under a magnetic field with $B = 1$ T[29b].

64 N. Vaupotic, J. Szydlowska, M. Salamonczyk, A. Kovarova, J. Svoboda, M. Osipov, D. Pociecha and E. Gorecka, *Phys. Rev. E: Stat., Nonlinear, Soft Matter Phys.*, 2009, **80**, 030701(R).

65 I. Dierking, *Textures of Liquid Crystals*, VCH-Wiley, Weinheim, 2003, p. 8.

66 J. P. F. Lagerwall, F. Giesselmann and M. D. Radcliff, *Phys. Rev. E: Stat., Nonlinear, Soft Matter Phys.*, 2002, **66**, 031703.

67 Hence, the situation in the nematic phases of compounds **1/n** seems to be distinct from the cybotactic nematic phases of main-chain polymers where the line shapes can only be fitted to Gaussian curves which indicates more static clusters embedded in a nematic continuum[36c].

68 Textural transformations in the nematic phase region were also observed for 4-alkoxy benzoic acids and some oxadiazoles; A. Sparavigna, A. Mello and B. Montrucchio, *Phase Transitions*, 2006, **79**, 293; A. Sparavigna, A. Mello and B. Montrucchio, *Phase Transitions*, 2007, **80**, 987.

69 Y. Yang, V. P. Panov, A. Kocot, A. Lehmann, C. Tschierske and J. K. Vij, *Appl. Phys. Lett.*, 2009, **95**, 183304; M. Nagaraj, Y. P. Panarin, U. Manna, J. K. Vij, C. Keith and C. Tschierske, *Appl. Phys. Lett.*, 2010, **96**, 011106.

70 K. V. Le, M. Mathews, M. Chambers, J. Harden, Q. Li, H. Takezoe and A. Jakli, *Phys. Rev. E: Stat., Nonlinear, Soft Matter Phys.*, 2009, **79**, 030701.

71 The influence of the magnetic field on the size of cybotactic clusters was previously proven by X-ray investigations, see ref. 29*b*. Hence, it is possible that the individual clusters might line up to strings (ribbons) or parallel sheets under the influence of the alignment field, see also: L. V. Azaroff, *Proc. Natl. Acad. Sci. U. S. A.*, 1980, **77**, 1252.

72 A. Lesac, H. L. Nguyen, S. Narancic, U. Baumeister, S. Diele and D. W. Bruce, *Liq. Cryst.*, 2006, **33**, 167.

73 B6 phases, which represent intercalated smectic phases, can be regarded as B1-type Col_r phases where the diameter of the ribbons is not fixed. This leads to a long range smectic order with only short range positional correlation of ribbons in the layers: S. Kang, M. Tokita, Y. Takanishi, H. Takezoe and J. Watanabe, *Phys. Rev. E: Stat., Nonlinear, Soft Matter Phys.*, 2007, **76**, 042701.

74 No good alignment is achieved by surface alignment; in this case only a ring corresponding to the small angle scattering is found in the temperature range of CybC phase, but no indication of the 2D lattice.

75 There is also the possibility of a change of the alignment of the bent aromatic core with respect to the magnetic field direction: V. Domenici, C. A. Veracini, K. Fodor-Csorba, G. Prampolini, I. Cacelli, A. Lebar and B. Zalar, *ChemPhysChem*, 2007, **8**, 2321.

76 H. J. Deutscher, R. Frach, C. Tschierske and H. Zaschke, in *Selected Topics in Liquid Crystal Research*, ed. H.-D. Koswig, Akademie-Verlag, Berlin, 1990, p.1.

77 S. A. Rama Krishnan, W. Weissflog and R. Friedemann, *Liq. Cryst.*, 2005, **32**, 847.

78 D. Demus and A. Hauser, in *Selected Topics in Liquid Crystal Research*, ed. H.-D. Koswig, Akademie-Verlag, Berlin, 1990, p.19.

79 Ethyl- and propyl-substituted bent-core molecules were previously reported for naphthalene based bent-core mesogens, but these compounds have nematic phases only in small temperature ranges at extremely high temperatures (200 °C)[42d].

80 Tetrahedric order in the nematic phases of the short chain compounds might provide an alternative explanation for their special XRD patterns, see: H. R. Brand and H. Pleiner, *Eur. Phys. J. E*, 2010, **31**, 37.